letnik/volume **53** - št./no. **4/07** - str./pp. **215 - 268**
Ljubljana, apr./Apr. 2007, zvezek/issue **504**

STROJNIŠKI VESTNIK

JOURNAL OF MECHANICAL ENGINEERING

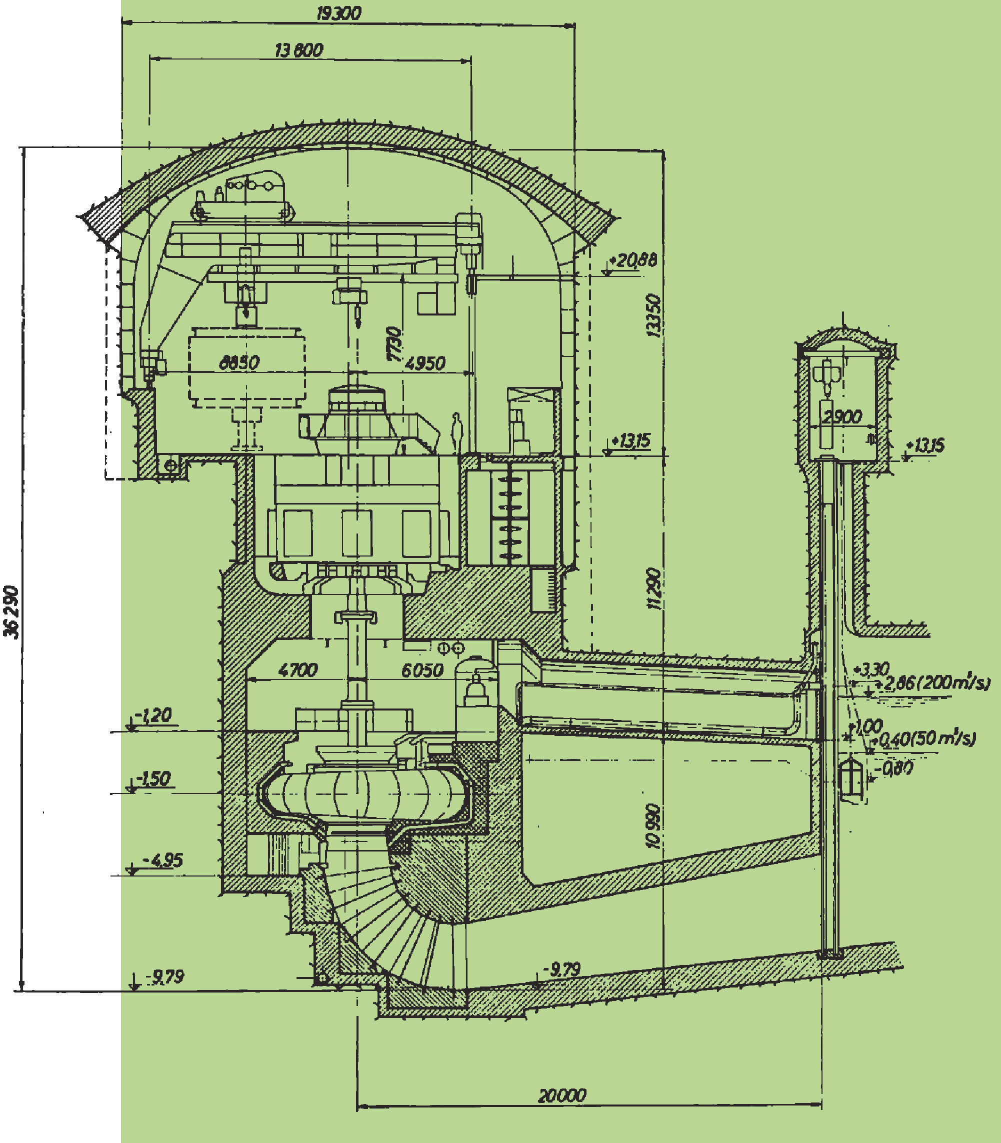

cena 3,34 EUR

9 770039 248001

ISSN 0039-2480

Vsebina - Contents

Strojniški vestnik - Journal of Mechanical Engineering
letnik - volume 53, (2007), številka - number 4
Ljubljana, april - April 2007
ISSN 0039-2480

Izhaja mesečno - Published monthly

Strojniški vestnik - Journal of Mechanical Engineering 53(2007)4, 216-223
UDK - UDC 629.1.073:531.44
Pregledni znanstveni članek - Review scientific paper (1.02)

Vpliv lastnosti cestišča na zavorne lastnosti avtomobila

The Influence of Road Surface on an Automobile's Braking Characteristics

Edgar Sokolovskij - Robertas Pečeliunas
(Vilnius Gediminas Technical University, Lithuania)

V prispevku smo opisali rezultate raziskave zavornih lastnosti avtomobilov, opremeljenih s protiblokirnim zavornim sistemom (ABS) in brez njega. Predstavili smo vrednosti zaviranja avtomobila, od trenutka zaviranja do konca zaviranja, na suhi asfaltno-betonski površini, ki je bila nespremenjena med raziskavo. Prikazali in dokazali smo odvisnost zaviranja avtomobilov, opremljenih z ABS in brez njega, od začetne hitrosti vožnje. Predstavili smo tudi rezultate preizkusov zaviranja avtomobilov, opremljenih z ABS in brez njega, v zimskih razmerah, na ledu in snegu. Opisali smo tudi stične lastnosti in zaviranja avtomobilov pri zaviranju na drugih površinah cestišča.

(Ključne besede: avtomobili, parametri zaviranja, ABS, dinamika zavor)

The present paper describes the results of an investigation into the braking parameters of automobiles equipped with an antilock brake system (ABS) and without an ABS. The values of the automobile deceleration, the time of the deceleration increase and the time of disbraking, while braking on a dry asphalt-concrete surface, which has been fixed in the course of the experimental investigation, are presented. The dependence of the deceleration of the automobiles, equipped with an ABS and without an ABS, upon the primary driving speed is reflected and substantiated. The results of the investigation of the braking of the automobiles, equipped with an ABS and without an ABS, in winter conditions, i.e., on ice and snow, are presented. The cohesion characteristics and the automobile decelerations while braking on other road surfaces are presented.

(Keywords: automobiles, braking parameters, ABS, dynamics)

0 INTRODUCTION

It is usual for the values of braking parameters, fixed for earlier models of automobiles, to be specified in reference sources [1]; however, these values are not usually appropriate for modern automobiles. The values of the braking parameters for automobiles specified in some sources do not match the modelling of the automobiles' movement. For example, the values for the deceleration of automobiles, specified by the manufacturers of automobiles and tires, are usually fixed for the phase of the most efficient braking, having not evaluated certain constituents of the braking process, as a result of which larger values are obtained. These values are, nevertheless, good for advertising and a comparison of products. However, for modelling the automobiles' movement (for example, for an examination of traffic accidents), values of the average, settled deceleration are necessary ([1] and [2]). Moreover, in the course of the investigation of the braking process, the deceleration of vehicles and the braking track are usually fixed; however, other parameters, such as the time of the deceleration increase and the time of disbraking, are also important when examining road-traffic accidents.

Recently, issues associated with antilock brake systems (ABSs), installed in automobiles, have frequently been considered, both in the scientific and popular references ([3] to [9]). However, so far not all the issues have been solved. The results of the investigation of the braking parameters and the peculiarities of the automobiles equipped with ABS, and of the automobiles without an ABS, are specified below [10].

1 METHODS AND CONDITIONS OF THE EXPERIMENTAL INVESTIGATION

The experimental investigation was carried out under the following conditions:

- cars, equipped with an ABS and without it, which were produced in the years 1986 to 2000 were used for the investigation;
- the cars were in a good mechanical condition and equipped with their factory (non-substituted) brake systems;
- two people served as the load in the tested cars, i.e., the driver and the "passenger", who was taking care of the measuring device (the decelerometer);
- the same person drove the car during all the tests;
- the cars were equipped with tires of the size that is recommended for the particular type of model; the depth of the protector notch was not less than 3 mm. The cars, equipped with summer tires, were tested on the dry surface of an asphalt road, whereas the cars equipped with the winter "non-prickly" tires were tested in winter conditions (on snow and ice);
- the air pressure of the tires was nominal for the particular model of car and its load;
- the tests were carried out on a horizontal strip of a "non-rough" asphalt road, where there was no traffic, by calculating the mean number later;
- the tests were carried out in both directions – not less than three tests in each case, by calculating the mean number later;
- in the course of the investigation of the dependence of the deceleration on the car's primary speed, the tests on the dry surface of the asphalt road were carried out with the cars equipped with the ABS, which were driven at a primary speed of 60 km/h, 80 km/h and 100 km/h, and with the cars without the ABS, which were driven at a speed of 30 km/h, 50 km/h and 80 km/h (for the sake of safety, the tests with the cars without the ABS were carried out at the lower primary speed);
- for the sake of safety, in the course of the investigation of the influence of the ABS's functioning on the car's deceleration in winter conditions, the cars driven at the primary speed of 30 km/h were tested in winter conditions (on the snow and ice).

Measurements were taken with the help of an electronic device that measures the deceleration, i.e., a VZM 100 decelerometer.

2 RESULTS OF THE EXPERIMENTAL INVESTIGATION

At first, the dependence of the deceleration of the vehicles without the ABS on the primary speed was investigated. The results of the investigation are presented in Fig. 1.

As we can see, the deceleration of the vehicle without the ABS decreases with the increase of the primary speed.

An analogous investigation was carried out with vehicles equipped with the ABS. The results of these investigations are presented in Fig. 2.

It must be stated that in the course of the testing the average settled deceleration of all the vehicles equipped with the ABS on the dry surface of the asphalt road was not less than 8 m/s^2 – it was within the range from 8 m/s^2 to 8.8 m/s^2. The vehicle's deceleration at the stage of the most efficient braking in most cases exceeded 9 m/s^2, sometimes it reached the value of the acceleration due to gravity (9.81 m/s^2).

In the course of the investigation it was observed that during the braking of the vehicles equipped with the ABS, it was sometimes difficult to observe the traces of braking of the wheels (especially in certain lighting conditions). However, in most cases the length of the remaining traces is shorter than the length of the braking path.

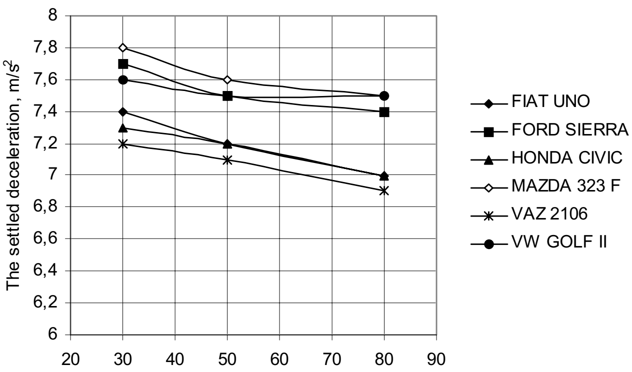

Fig. 1. *Dependence of the deceleration on the primary speed during the braking of vehicles without the ABS*

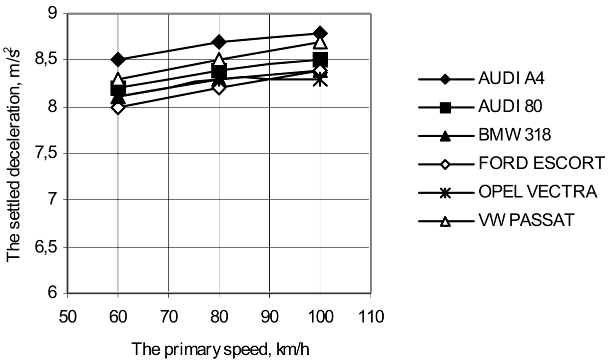

Fig. 2. *Dependence of the deceleration on the primary speed during the braking of vehicles equipped with the ABS*

It was ascertained that during the braking of the vehicles equipped with the ABS, the deceleration does not decrease; it even increases with the increase of the primary speed of the vehicle. In order to explain this situation, we will compare the braking diagrams in both cases (Fig. 3).

As it is clear from the braking diagram that the deceleration of the vehicle without the ABS, which is in a good mechanical condition, reaches its peak at the very beginning of braking, during which time the vehicle's wheels continue to rotate. When the wheels become locked, the deceleration decreases to a certain extent because the braking of a locked wheel is less efficient (Fig. 3, b). Thus, in the course of braking for the vehicle without the ABS, when the vehicle is driven at a lower speed, the above-mentioned peak of deceleration makes a larger part of the whole process of braking and in contrast the peak makes up a smaller part of the process of braking when the vehicle is driven at a higher speed and the process of braking takes a longer time. In addition, the other factors, such as the heating of the tire compound of the blocked wheel of the automobile in the contact zone, etc., are also significant. The deceleration decrease, typical of the vehicles that are driven at the increasing primary speed, can be explained by this fact. It should be noted that it was not always the "classic" diagrams of braking, reflecting the peak in the maximum deceleration, when starting to brake that were obtained in the case of braking for the automobiles without the ABS.

In the course of braking for the vehicles equipped with the ABS (according to the principle of the ABS the wheels remain unlocked during the whole period of braking), there is no deceleration peak at the beginning of braking. On the contrary, in the course of braking for the vehicles equipped with the ABS, when the wheels interact with the surface of the road (the ABS controls the situation and prevents the wheel slip from exceeding a certain value –

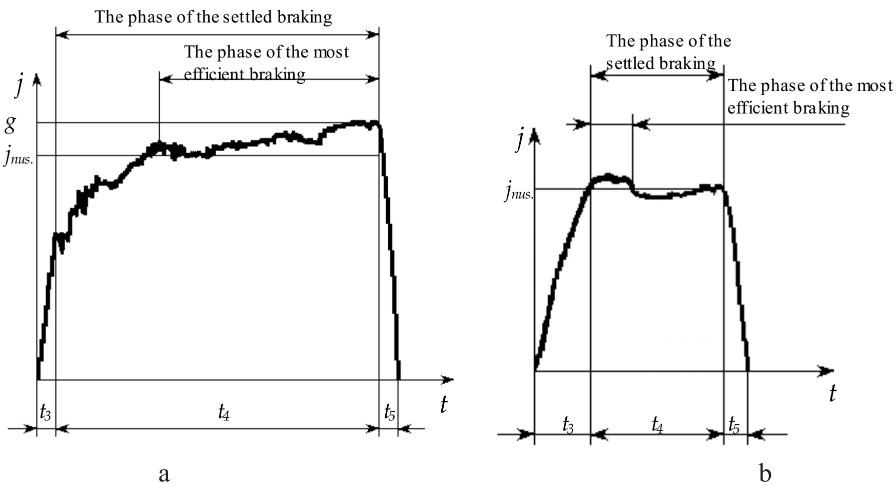

Fig. 3. *The diagrams of braking: a – the vehicle equipped with the ABS, b – the vehicle without the ABS*

Table 1. *The time of deceleration increase, t_3, and the time of disbraking, t_5*

Vehicle	***ABS***	***Time of deceleration increase t_3, s***	***Time of disbraking t_5, s***
AUDI A4	+	0.1	0.1
AUDI 80	+	0.15	0.1
BMW 318	+	0.15	0.1
FIAT UNO	–	0.2	0.15
FORD ESCORT	+	0.15	0.15
FORD SIERRA	–	0.2	0.1
HONDA CIVIC	–	0.25	0.15
MAZDA 323 F	–	0.2	0.1
OPEL VECTRA	+	0.15	0.15
VAZ 2106	–	0.3	0.2
VW GOLF II	–	0.2	0.1
VW PASSAT	+	0.1	0.1

usually, approximately 20%), the deceleration continues to increase insignificantly in the course of further braking after the phase of increase for the deceleration. Thus, slightly smaller deceleration values are reached at the beginning of braking, whereas the largest values are usually reached when the process of braking becomes stable at the end of braking. The deceleration increase with the increase of the primary speed of the vehicle equipped with the ABS can be explained by this fact (Fig. 3, a).

Furthermore, the values of the time of the deceleration increase, t_3, and of the time of disbraking, t_5, were determined in the course of the investigation. The obtained results are presented in Table 1.

As we can see, the values of the time of deceleration increase, t_3, for all the vehicles that were investigated did not exceed 0.3 s. This value was typical for the VAZ 2106 automobile. The values of the time of deceleration increase, t_3, for most of the Japanese and western vehicles did not exceed 0.2 s and remained within the limits of 0.1 to 0.2 s. The only exceptions were very old-fashioned vehicles. In this case it was a 15-year-old HONDA CIVIC, which achieved a value of 0.25 s.

The values of the disbraking time, t_5, specified in certain written sources that were published earlier were not proven (for the hydraulic brake system $t_5 = 1.5\, t_3$). The values of the time of disbraking, obtained in the course of the investigation did not exceed the values of the time of deceleration increase and were within the limits of 0.1 to 0.15 s, except for the VAZ 2106, with the time of disbraking equal to 0.2 s.

Braking tests were also carried out in winter conditions, i.e., on ice and snow. For this we used a FORD ESCORT (equipped with the ABS) and a FORD SIERRA (without the ABS). The obtained results are presented in Table 2.

In the course of the investigation it was determined that a slightly higher deceleration was typical for the vehicle equipped with the ABS (FORD ESCORT) when braking on the ice.

Slightly different results were obtained when braking with vehicles equipped with the ABS and without it on a snowy road surface, fit for traffic. In this case a slightly higher deceleration was typical for the vehicle without the ABS (FORD SIERRA). Such unexpected results can be explained by the fact that the locked wheels of the vehicle without the ABS contact the wet surface of the asphalt road, covered with a thin layer of snow, thus causing the deceleration increase. In addition, the locked wheels

Table 2. *Deceleration of the vehicles equipped with the ABS and without it, in winter conditions*

Surface of the road, fit for traffic	***Average deceleration of the vehicle, equipped with the ABS (FORD ESCORT), m/s^2***	***Average deceleration of the vehicle without ABS (FORD SIERRA), m/s^2***
Ice	2.0	1.8
Snow	2.6	3.0

push and thicken the snow in front of them. Thus, the area of the wheel pressure increases and the effect, similar to the braking of the vehicle on a soft surface (for example, soft soil) reveals itself.

The wheels of the vehicle equipped with the ABS remain unblocked. Thus, they do not contact the wet surface of the asphalt road and the deceleration is lower. However, it should be stressed that in any case, including the case when braking the vehicle on the snow (though in this case the deceleration of the vehicle equipped with the ABS was a bit lower), the ABS has a significant positive influence on the operation of the vehicle as the possibility to drive the vehicle remains. This is very important for traffic safety as most traffic accidents occur because it is not possible to correctly operate the vehicle.

3 COHESION CHARACTERISTICS AND AUTOMOBILE DECELERATION WHILE BRAKING ON THE DIFFERENT ROAD SURFACES

A vehicle is driven along various road surfaces. Sometimes a situation occurs when there are places on the road fit for traffic where the coefficient of cohesion of the surfaces with the wheels is different ([11] to [18]). For example, the surface of the road, fit for traffic, is covered with sand or slush, is coated with ice in certain places, etc. Furthermore, the values of the deceleration of the vehicles and the cohesion coefficients of their wheels while braking on different road surfaces in each definite case will be submitted. Such data are necessary while analysing and modelling the vehicle's movement under various road conditions, while restoring the course of traffic accidents and while carrying out an examination of traffic accidents.

The diversity of road surfaces is vast in winter conditions. For example, the statement that a stretch of the road, fit for traffic, is covered with snow points to almost nothing. It may mean snow that has just fallen; snow that is churned up; snow that is covered with a layer of ice; churned up snow that is covered with sand, etc. Accordingly, the coefficient of cohesion of the wheels with the road surface is different in each case.

Some values of deceleration in winter conditions are included in Table 2. However, sometimes cases that have not been described in the literature

Table 3. *Coefficient of cohesion on snow and ice*

Road surface	***More detailed description of the surface condition***	***Coefficient of cohesion, φ***
Churned up snow	Snow, churned up by vehicles, which does not make a compounded layer of snow and ice	0.24 to 0.37
Non churned snow	Snow that has just fallen on the asphalt and that is not churned up with the wheels of vehicles – the first drive	0.15 to 0.42
Snow and ice, covered with the snow that has just fallen	Churned up snow and ice, covered with a layer of snow (thickness – up to10 cm), which has just fallen and is not churned up	0.18 to 0.45
Snow and ice, mixed with sand and slush	Churned up snow and ice, mixed with sand and slush, the particles of which are 3 to 6 mm in diameter	Depending upon the quantity of slush (little – much) 0.15 to 0.45
Snow and ice	Entire layer of snow, churned up to reveal the icy surface	0.12 to 0.39
Snow and ice before crossroads	Snow, which first was melted by the motors of the standing vehicles and then frozen to produce a smooth surface	0.09 to 0.22
Deep snow	Deep and non-touched snow when the vehicle "seats itself on the bottom"; however, it does not stick	0.92 to 0.95
Dry asphalt in winter conditions	Dry asphalt (uncovered with anything) in winter conditions	0.59 to 0.72
Asphalt, covered with hoar-frost	White cover on the asphalt, which is observed by the driver and easily recognized as hoar-frost	0.48 to 0.58
Smooth ice	Thick layer of frozen water, not penetrated by spikes and chains	0.054 to 0.19
Ice and tires with chains	Thick non-penetrated layer of frozen water, penetrated by wheels equipped with steel chains	0.12 to 0.18
"Black" ice	Thick ice layer that looks like a wet, black stretch of road, which is fit for traffic, but which is not easily noticed by the driver	0.12 to 0.26

Table 4. *Values of deceleration for a vehicle while braking on various non-typical surfaces ([10], [13] to [16])*

Road surface	***Deceleration***
Churned up soil	(0.6 to 0.65) *g*
Grass	(0.35 to 0.54) *g*
Sand, gravel (loose – compounded)	(0.4 to 0.7) *g*
Edge of the road (non-asphalted)	(0.35 to 0.4) *g*
Slush on a wet surface	(0.2 to 0.3) *g*

Remark: *g* is the acceleration due to gravity, m/s^2.

occur in practice. The values of the coefficient of cohesion on the snow and ice are listed in Table 3. These values pertain to universal tires.

It is a common case that the values of the coefficient of cohesion that are listed in the literature for such cases differ, or their limits are too wide. It is like this because the conditions of the investigation, the type of tires, the model, etc., significantly influence the obtained values. It is known that the snow and ice change their qualities depending upon the temperature. Thus, this fact influences the obtained results.

The values of the deceleration of vehicles while braking along various non-typical surfaces, which are specified in the literature ([10], [13] to [16]), are listed in Table 4.

Sometimes, very unusual surfaces, which are not typical for normal traffic, occur. However, practically (for example, while carrying out the examination of traffic accidents), such data, that may be applied to individual cases, are necessary as well. Thus, Table 5 reflects the deceleration of a vehicle with ABS while braking on wet asphalt, which is covered with grain [17]. The deceleration was measured exactly on the wet asphalt because, from the point of view of traffic safety, such a case is more dangerous because at that time a significant reduction in the deceleration is observed (similar to the braking on the asphalt, which is covered with slush).

Table 6 reflects the deceleration of the automobile while braking on the asphalt, which is covered with motor oil or resin ([11], [13] to [16]).

Table 5. *Deceleration of a vehicle with ABS while braking on a wet asphalt surface, covered with a layer of grain [17]*

Road surface	***Deceleration, m/s^2***
Wet asphalt, covered with a "dry" layer of grain	3.3
Wet asphalt, covered with a "wet" layer of grain	2.9

Interesting results were obtained while investigating the deceleration of a vehicle while braking on a stretch of road, fit for traffic, on which petrol was spilt ([11] and [18]). The dependence of the deceleration on the time (when the surface was drying) was investigated. The results of the investigation prove that the spilt petrol immediately starts to react chemically with the asphalt and creates a very slippery surface, which later dries and acquires the previous coefficient of cohesion. The surface of the stretch of the road, fit for traffic, being wet with water in the place where the petrol was spilt has a slightly smaller coefficient of cohesion. The results of the investigation are listed in Table 7.

The investigation proves that the deceleration of the vehicle with the up-to-date tires when the wheels slide in the transversal direction is close to the value of deceleration while braking on the same surface [19].

4 CONCLUSIONS

1. In the course of braking for vehicles equipped with the ABS, on the dry surface of an asphalt road, the average settled deceleration was within the limits from 8 m/s^2 up to 8.8 m/s^2; in most cases the deceleration exceeded 9 m/s^2 in the phase of the most efficient braking. The values of the time of the deceleration increase, t_3, typical for the vehicles equipped with the ABS were within the limits 0.1 to 0.15 s. The values of the time of disbraking, t_5, did not exceed the time values of

Table 6. *Deceleration of the vehicle while braking on asphalt covered with motor oil or resin ([11], [13] to [16])*

Road surface	***Deceleration***
Wet, rough asphalt, on which oil is spilt	(0.25 to 0.3) *g*
Wet, smooth asphalt, on which oil is spilt	(0.05 to 0.12) *g*
Resin is spilt on the asphalt	(0.5 to 0.64) *g*

Table 7. *Deceleration of a vehicle while driving across a petrol spill ([11] to [18])*

Description of the surface and driving	***Time***	***Deceleration***
Driving along dry asphalt without a spill of petrol	–	0.8 *g*
Driving across the spill of petrol	After 10 s from the moment of spilling the petrol	0.22 *g*
Repeated driving across the trace	3 min after the spot became dry	(0.60 to 0.34) *g* (according to the direction of driving)
Repeated driving across the trace	6 min after the spot became dry	(0.80 to 0.54) *g* (according to the direction of driving)
Driving across the non-driven spill	9 min after the spot became dry	0.56 *g*
Driving across the completely dried spot	25 min	0.80 *g*
Driving on the wet asphalt without the spill	–	0.55 *g*
Driving across the spill of petrol on wet asphalt	50 min after the moment of spilling	0.45 *g*

the deceleration increase and were within the limits 0.1 to 0.15 s.

2. The average settled deceleration of the vehicles without the ABS, while braking on the dry surface of an asphalt road, were within the limits from 6.9 m/s^2 up to 7.8 m/s^2. The values of the time of the deceleration increase, t_3, were within the limits 0.2 to 0.3 s. The values of the time of disbraking, t_5, did not exceed the time values of the deceleration increase and were within the limits 0.1 to 0.2 s.
3. It was determined that during braking for the vehicles equipped with the ABS the average settled deceleration increases with the increase of the primary speed of the vehicle, whereas in the case of braking for the vehicles without the ABS, it decreases (Figs. 1 and 2). This significant difference, typical of the vehicles equipped with the ABS and the vehicles without it, is reflected in the diagrams of braking (Fig. 3).
4. After having carried out the experimental investigation in winter conditions, it was determined that the automobile equipped with the ABS braked on the ice more efficiently (by approximately 10%). The vehicle without the ABS braked on the snow-covered surface of the road more efficiently (approximately 13%), because in this case the blocked wheels of the vehicle without the ABS contact the wet surface of the asphalt road, and so push and thicken the snow in front of them. However, in any case, the ABS plays a significant positive role in the control of the vehicle as the possibility to drive the vehicle remains.
5. The cohesion characteristics and the automobiles' decelerations while braking on different road surfaces are presented. There is a possibility to model the vehicles' movement and to restore the course of the traffic accidents more precisely while carrying out the examination of the traffic accidents. However, it is necessary to use the fixed values of the braking parameters of automobiles while evaluating the technical condition of the particular automobile as in certain cases (for example, dealing with old automobiles) these values may be unsuitable.

5 REFERENCES

[1] Иларионов В. А. (1989) Экспертиза дорожно - транспортных происшествий. *Москва: Транспорт*, 254 с.

[2] Lukoševičiene O. (2001) Autoivykiu analize ir modeliavimas. Monografija. Vilnius: *Technika*, 244 p.

[3] Ahlgrimm J., Grandel J. (1997) Verkehrsunfallaufnahme bei Fahrzeugen mit Anti-Blockier-System (ABS). *Verkehrsunfall und Fahrzeugtechnik*, No 3, 1997, p. 67–74.

[4] Bogdevičius M., Prentkovskis O., Vladimirov O. (2004) Engineering solutions of traffic safety problems of road transport. *Transport*, 2004, Vol XIX, No 1, p. 43–50.

[5] Danner M., Halm J. (1994) Technische Analyse von Verkehrsunfällen. *Eurotax (International) AG CH-8808* Pfäffikon, 570 p.

[6] Mills V., Samuel B., Wagner J. (2002) Modeling and analysis of automotive antilock brake systems to Vehicle Payload Shifting. *Vehicle System Dynamics*, Vol 37, No 4, 2002, p. 283–310.
[7] Sherman D. (1998) The ABCs of ABS. *Popular Science*, Vol 252, No 6, 1998, p. 75–79.
[8] Donges E. (1999) A Conceptual framework for active safety in road traffic. *Vehicle System Dynamics*, Vol 32, No 2/3, 1999, p. 113–128.
[9] Lewandowski A. (2000) Czynniki decydujące o skuteczności hamowania samochodu z ABS. In: *Proceedings of the 7th conference "Problems of reconstruction of road traffic accidents"*. Krakow, 11–12 September, 2000. K.:IES, p. 227–237.
[10] Sokolovskij E. (2004) Rato saveikos su keliu ir jo elementais tyrimai eismo ivykiu ekspertizes kontekste. Daktaro disertacija. *Vilnius: VGTU*, 147 p.
[11] Unarski J., Wach W., Zębala J. (2000) Przyjmowanie wartości współczynnika tarcia w różnych szczególnych okolicznościach. *7 konferencja. Problemy rekonstrukcji wypadków drogowych*. Kraków, 11–12 września. K.:IES, 2000, s. 255–265.
[12] Martin D. P., Schaefer G. F.: Tire-road friction in winter conditions for accident reconstruction, Society of Automotive Engineers, Inc., *SAE Paper 969657*.
[13] Christofferson S., Jarzombek M., Wallingford J.: Deceleration factors on off-road surfaces applicable for accident reconstruction, Society of Automotive Engineers Inc., *SAE Paper 950139*.
[14] Fricke L. (1990) Traffic accident reconstruction, *Northwestern University Traffic Institute*.
[15] Limpert R. (1989) Motor vehicle accident reconstruction and cause analysis, *The Michie Company*.
[16] Collins J. C. (1979) Accident reconstruction, *Charles Thomas*, Springfield.
[17] Anioła M., Kurek J., Lewandowski A., Warszczyński J. (2000) Hamowanie samochodu osobowego w warunkach zagrożenia bezpieczeństwa, wywołanego zmianą stanu nawierzchni. *7 konferencja. Problemy rekonstrukcji wypadków drogowych*. Kraków, 11–12 września. K.:IES, 2000, s. 219–227.
[18] Grandel J.: Untersuchung des Einflusses von Benzin auf die Griffigkeit einer Asphaltbetonfahrbahn, Der Verkehrsunfall 11/91, *Ambs Verlag*.
[19] Navin F., Macnabb M., Nicoletti C.: Vehicle traction experiments on snow and ice, Society of Automotive Engineers, Inc., *SAE Paper 960652*.

Authors' Address:
Doc. Dr. Edgar Sokolovskij
Doc. Dr. Robertas Pečeliunas
Vilnius Gediminas Technical University
Dept. of Automobile Transport
J. Basanavičiaus 28, LT-03224
Vilnius, Lithuania
edgar.sokolovskij@ti.vtu.lt
robertas.peceliunas@ti.vtu.lt

Prejeto: 6.12.2006
Received:

Sprejeto: 21.2.2007
Accepted:

Odprto za diskusijo: 1 leto
Open for discussion: 1 year

Strojniški vestnik - Journal of Mechanical Engineering 53(2007)4, 224-232
UDK - UDC 621.794.4:535.08
Kratki znanstveni prispevek - Short scientific paper (1.03)

Raziskave vodno jedkanih površin s svetlobnim zaznavanjem

An Investigation of Surfaces Generated by Abrasive Waterjets Using Optical Detection

Jan Valíček[1] - Sergej Hloch[2] - Milan Držík[2] - Miloslav Ohlídal[3] - Vilém Mádr[1] - Miloslav Lupták[4] - Agáta Radvanská[5]
([1]Technical University of Ostrava, Czech Republic; [2]Slovak Academy of Sciences; [3]Brno University of Technology, Czech Republic; [4]Faculty of Metallurgy of Košice, Slovak Republic; [5]Technical University of Košice, Slovak Republic)

V prispevku smo opisali načelo nove metode svetlobnih meritev vodno jedkanih površin. Definirali smo paramatre meritev in določili postopek ustvarjanja podatkovne baze izmerjenih vrednosti ter metodo statistične in analitične obdelave podatkov za optimiranje tehnologije, izboljšanje kakovosti nadzora izdelave ter proučevanje mehanizma razkroja medsebojnega vpliva jedkalnega vodnega curka z velikimi hitrostmi in obdelovanega materiala.

(Ključne besede: jedkanje površin, abrazivni vodni curek, površinska hrapavost, optične meritve, spektralne analize)

In this paper we describe the principle of a new method for the optical measurement of surfaces generated by abrasive waterjets. There measured parameters are defined and we determined the way of creating a database of the measured values, and the method for statistical and analytical processing of data for optimising the technology, improving the quality of output control, and studying the mechanism of disintegration interaction between the high-speed abrasive waterjet and the machined material.

(Keywords: abrasive waterjet, surface roughness, optical measurement, spectral analysis)

0 INTRODUCTION

In the engineering practice of machinery, recent decades have been characterized by the intense development of non-traditional technologies in the machining of materials, including many technologies for machining using high-speed jets of liquid, especially those that involve the use of highly abrasive materials. While the technology of machining using a high-speed jet has already been solved in terms of hardware and software (except for some specific cases), the method of controlling the quality of the machined surfaces has remained a technical problem. The paper deals with the problems of selecting and proposing an acceptable method for surface-quality control that is available for continuous measurement and production. Knowledge of the surface topography and classification is very important for the machining techniques and research.

1 RELATED WORKS

The scale of the basic metrology operations is defined by standards determining a required quality class. These operations lead to the correct results for surfaces created by traditional technologies. The physical basis of the formation of new surfaces by non-conventional technologies is different; therefore, the geometrical characteristics of the created surface will be different ([1] and [2]). Surfaces produced by the technology of abrasive waterjets (henceforth referred to as AWJs) are very rough in comparison with those generated by classical machining technologies. The amplitudes of irregularities in terms of height are comparable with the amplitudes of these irregularities on more roughly dressed or planed surfaces. In comparison with ground, polished and lapped surfaces, those reach values can be even two orders of magnitude higher. With reference to the flexibility of a cutting tool, which is a high-speed stream of a mixture of water, abrasive particles and air, cutting traces are intensively curved in this case, and any constant spacing is not maintained. The lagging of the cutting traces behind the nozzle causes a specific deformation in the entry initiation and also the exit zone, i.e., greater deformation of the marginal edges of the samples. The changes in the direction of the vector of the total cutting force have an oscillating character with a frequency depending upon the materials, the cut length, or cut depth. Oscillations in the total cutting force and its components manifest themselves fully in the character of the distribution of the geometrical parameters of the final surface topography. The described specifics of these surfaces require specific approaches to the measurement methodology and interpretation. That is why our work was focused on the development of a new, optical-principle-based measurement apparatus, further on a definition of and the requirements for the optical quantity measured, on the structured selection of surface parameters measured, and on the way of storing the data and processing.

2 PROBLEM DEFINITION

Fig. 1 presents a photograph of a surface produced by AWJ, including the division into individual specific zones, i.e., the initiation zone (h_I), the smooth (h_{II}), transition (h_{III}) and rough (h_{IV}) zones. Next, surfaces created like this must be controlled, and the AWJ technology parameters must be influenced to increase the quality of a cut. As can be seen in Fig. 1, this surface is very rough and, in contrast to classically formed surfaces that have a mirror-like reflection, this surface is diffusion reflecting. For this reason, it is necessary to search for a way of measuring such specific surfaces. Another problem is the selection of the characteristic geometrical parameters of the topography structure. In Fig. 1 is the photograph of, and the proposal for, geometrical parameters typical of surfaces produced by AWJ. The statistical and analytical procedure prepared by us for the processing of data measured tends, from the point of view of conception, to derive physical equations for the relationships between the individual topographic parameters and the technology quantities.

3 PROBLEM SOLVING

3.1 Experimental Setup

A two dimensional AWJ machine Nessap 1000-V with the following specification was the main part of the experimental setup: the work table, x-axis 800 mm, y-axis 1000 mm, z-axis, discrete motion with a maximum traverse speed of 250 mm.min^{-1}. A PTV-37-60 high-pressure intensifier pump with a maximum pressure of 415 MPa and a Paser III cutting head manufactured by Flow Inc. were used. The basic technological parameters are presented in Table 1.

From the prepared metal plates of materials AISI 309, Fe 430 D2, Fe 360 BFN, GS 21 Mn5, AlMg, Zn, Al, brass and duralumin of thickness 8 mm, test samples of the dimensions (20 x 20 x 8) mm were cut out (see Fig. 2), with all the edges of the given sample being formed at different speeds (200, 150, 100 and 50 mm.min^{-1}). The height of 8 mm of each sample tested was measured by the optical shadow method

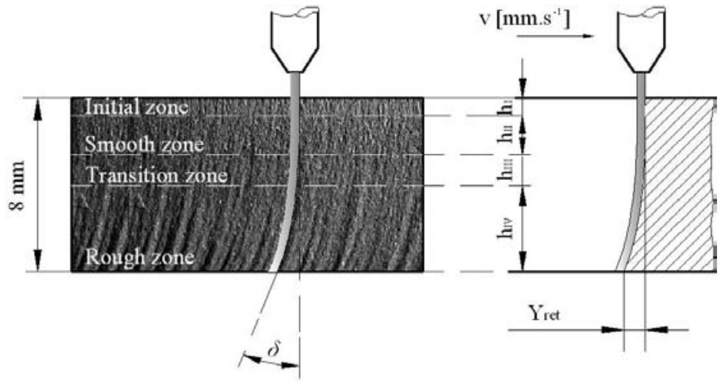

Fig. 1. *A photograph of a surface produced by AWJ with specific zones, i.e., initiation (h_I), smooth (h_{II}), transition (h_{III}) and rough (h_{IV}) zones, and the proposed main parameters of the surface profile, where δ is the angle of deviation, Y_{ret} is the retardation of the cutting trace over the height of sample h = 8 mm.*

Tabel 1. *Experimental setup*

Constant factors	Values	Constant factors	Values
Pressure p [MPa]	300	Standoff L [mm]	2 mm
Nozzle diameter d_o [mm]	0.25	Abrasive material	Barton Garnet
Focusing tube diameter d_a [mm]	0.8	Mesh [#]	80
Focusing tube length l_a [mm]	76	Cutting head	Flow Inc. Paser III.
Abrasive mass flow rate m_a [g.min^{-1}]	250	Variable factors	Values
Material thickness h [mm]	8	Traverse speed v_p [mm.min^{-1}]	50, 100, 150, 200
System characteristics of PTV-37-60 Pump			
Intensifier type	Double effect	Water pressure (max)	415 MPa
Electric input	37 kW	Water discharge (max)	3.68 l.min^{-1}

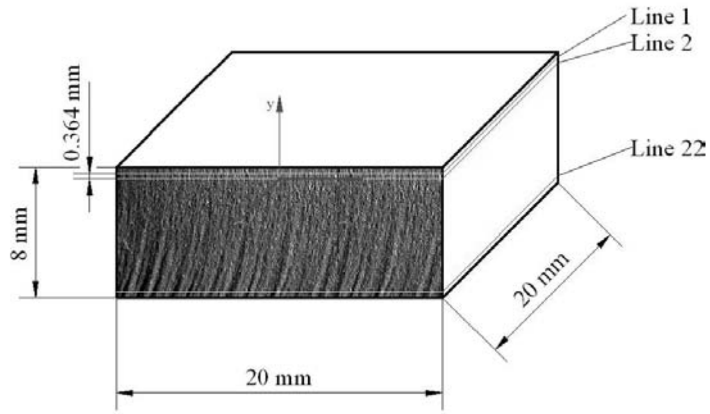

Fig. 2. *A test sample and measuring traces*

based on a CCD camera. The measurements were performed along 22 measuring lines at a vertical step of 0.364 mm on 4 walls. The soft materials, such as AlMg, pure Al and Zn, were machined at double the speed in the sequence of 400, 300, 200 and 100 mm.min^{-1} on these walls.

4 MEASUREMENT PROCEDURE

The quality of the surface of each wall of samples was measured by the optical method using a CCD camera along 22 geometrical traces with a vertical step of 0.364 mm (Fig. 3). The experiments were performed with both the laser light and the incoherent white light to test the possibilities of the light sources. In addition, the profound analysis was done to optimise the angle of illumination of the surface being measured. Despite its principal simplicity, the method takes into account the real information about the distribution of the surface roughness and also the elongated character of the surface defects. Thus, to all appearances, the measurement principle is appropriate for the purpose of studying the AWJ-created surfaces. At present, a CCD camera with 1090 x 1370 pixels is used for sensing and recording the intensity distribution of the light reflected off the surface. The experiments were carried out by using a laser diode with an output power of 3 mW at a wavelength of 650 nm. The surface observed is illuminated at a small, oblique angle by a beam of collimated light. The shadow visualisation effect arises from a change in the surface reflectivity with the illumination angle. Using this kind of illumination, hills, dimples and other defects and the typical waviness created by the AWJ are easily observable. Next, correct information about the surface quality can be obtained using a fast Fourier transform (FFT). After the FFT we obtain a frequency spectrum. The optical signals of the light and shadow surface distribution were analysed with the aim of obtaining the *RMS* (root mean square) of the intensity of the light reflection from the surface and transforming the equations between the *RMS* and the surface-roughness parameters, particularly the average roughness, *Ra* [μm].

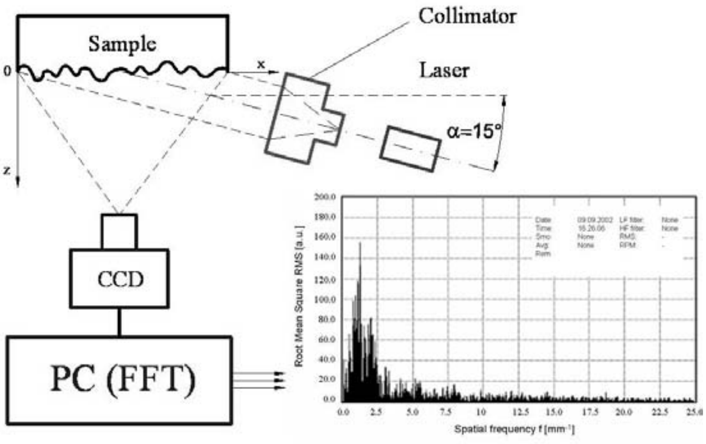

Fig. 3. *Basic setup for the optical method of shadow visualisation by CCD camera*

Along separated horizontal traces, selected geometrical parameters were measured optically as light-intensity variations. As the main surface geometrical parameters the average roughness, *Ra* [µm], the stream deflection, Y_{ret} [mm], and the deviation angle, δ[°], were proposed, see Fig. 2. The character of the distribution of the topographic elements divided the surfaces generated by the AWJ into the cutting wear zone, h_c [mm], and the deformation wear zone, h_d [mm], according to [3] and [4].

The values of the intensity distribution from the horizontal lines were projected into a CCD chip, and thus converted into the sample heights' distribution. On the basis of the statistical analyses, basic equations of the correlation with the measured optical quantity *RMS* (root mean square of the intensity of the light reflection from the surface) and to the cut depth *h*, defining the geometrical parameters of the surface were physically derived [5]. The parameters are presented in Figs. 4, 5 and 6.

The fluctuation in the *RMS* parameter depending on the topographic properties and the depth is shown in Figure 7. By the conversion of the *RMS* values to *Ra* values we obtain a characteristic view of the development of the roughness, *Ra*, the retardation, Y_{ret} , and the deviation, δ, depending on the cut depth, *h*.

5 RESULTS AND DISCUSSION

Fig. 8 presents the results achieved with a HOMMEL TESTER T8000 contact profilometer, i.e.,

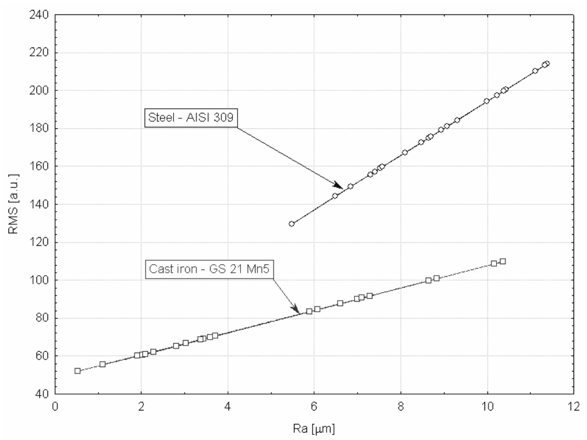

Fig. 4. *Parameter of roughness, Ra, for steel AISI 309: Ra = 0.07RMS-3.6 and Ra for cast iron GS 21 Mn5: Ra = 0.17RMS-8.3, determined by the conversion from the RMS according to the presented relations*

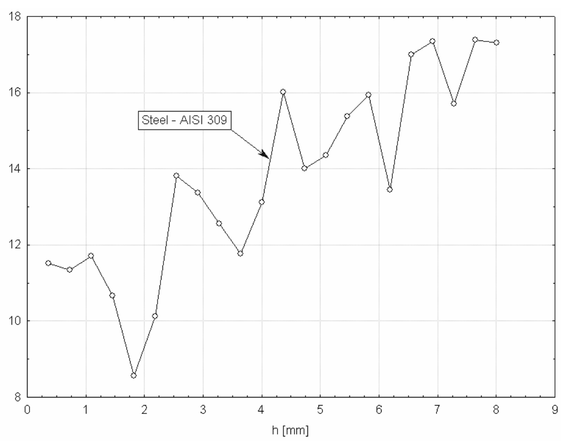

Fig. 5. *Deviation angle δ, δ= arctg(Yret/h)*

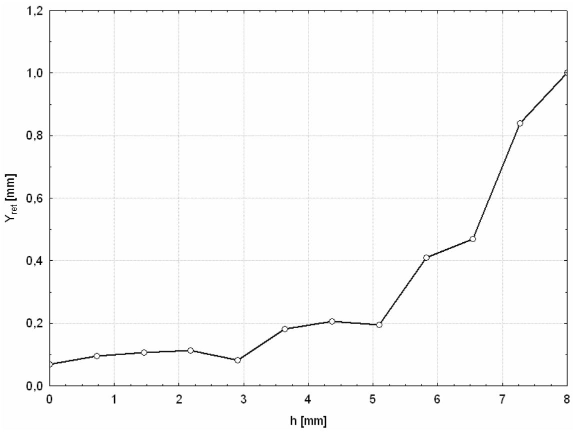

Fig. 6. *Stream deflection $Y_{ret:}$, $Y_{ret:} = 0.222.Ra.h_{rel}$, where the relative depth $h_{rel} = h_i/h$, h_i is the value of the trace depth at a cut level*

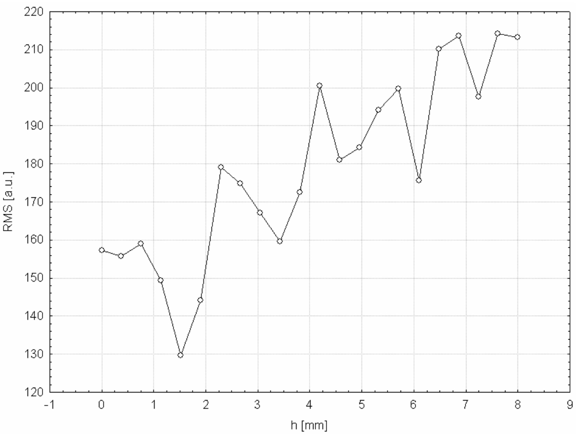

Fig. 7. *Dependence of RMS on the cut depth h for steel AISI 309*

a graph of roughness, *Ra*, versus the cut depth, *h*. These results show a good correspondence between the methods of direct measurement and those of optical measurement. Simultaneously, they draw attention to a serious fact concerning the problems of the detailed measurement of deformed sample edges in the initiation zone in a section Δh_x. This means that by using the contact profilometer the initiation zone with a higher roughness cannot be completely detected and localised. On the contrary, the results obtained with a MicroProf (FRT) optical profilometer show that more detailed information on the initiation zone can be provided. From the mechanical point of view, this entry region is of importance to the subsequent clarification of a mechanism of material removal and the explanation of AWJ-material interaction in this initiation zone (Fig. 9). From the practical point of view, it is then necessary to talk about impacts on the quality of the output control of the machined products. According to the results shown in Figure 8 and Figure 9, the initial zone is not identified by the contact profilometer, because the principle of measurement by means of a contact point does not allow any measurement in the immediate vicinity of the edge of workpiece when using the AWJ cutting technology. Improving the quality or the objectivization of the output control of the quality of the machined walls can thus be achieved by supplementing the contact measurement by optical detection.

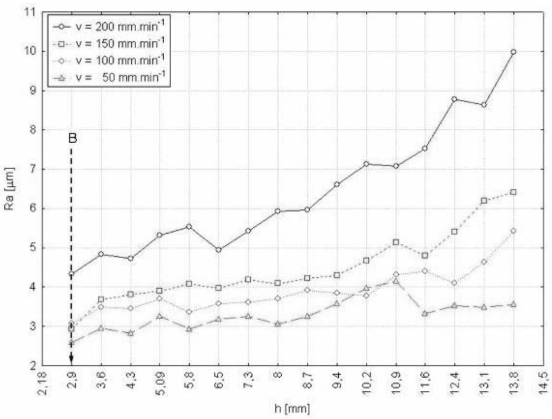

Fig. 8. *Results of the Ra measurement achieved with the contact profilometer, where B is the potential measurement beginning*

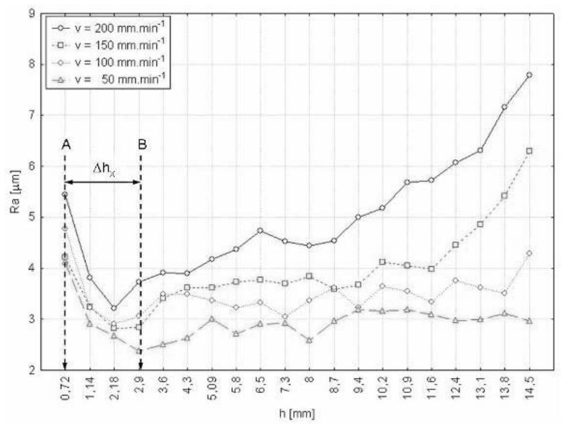

Fig. 9. *Results of the Ra measurement achieved with the optical method, where Δh_x is the difference between the points A and points B, representing an additionally measured surface*

From the analyses performed and from the obtained data (*RMS*, *Ra*, Y_{ret}, δ) on the surface topography, a mechanism for the formation of the surface topography, which is in fact a "memory" of the machining technology and also a "witness" to the properties of the material being machined can be deduced. For reasons of mechanical flexibility, and thus the ability of the AWJ tool to accommodate itself to the material properties, this tool is very suitable for a theoretical analyses. It is possible to say that in terms of the newly developed disciplines of technological inheritance, a profounder analysis of the process of surface-layer origin can be carried out. The authors Hashish, Bitter, Finnie ([3] and [4]) divide generated surfaces from the point of view of the removal mechanism into those with the removal mechanism of a cutting character and those with the removal mechanism of a deformation character. According to the literature [5], the topography formed is divided into the initiation zone (which is, however, neglected by the majority of authors), the smooth zone, and the rough zone. In our opinion, in the mechanism of the origin of a newly generated surface topography, the initiation zone cannot be ignored. This is the first contact with a disintegration tool, which here is a high-energy jet of a mixture of water, air and abrasive. In terms of a description of the AWJ's spread and degradation, it is possible to observe some phenomena (Figs. 10 and 11), i.e., the initiation zone, with a steep increase in the *RMS*, *Ra* values. Then, after exceeding the modulus of elasticity and overcoming the total resistance of the material in the initiation zone, there is a sharp drop in the *RMS*, *Ra* values. This phenomenon is related to the fact that a removed material from the sidewalls entered the jet when passing through the entry part of material, an abrupt oversaturation took place and also there was a contrast division of the jet structure into the inner core and the external envelope with a high concentration of abrasive grains lagging behind the inner core. In the external envelope, the kinetic component of the hydraulic energy transforms quickly to the potential energy, similarly to the case of hydraulic water shock. Using the potential energy excess, a deeper groove with a rather smooth trace will be formed, to which the optical device will respond with a decrease in the *RMS* value due to a low *Ra* value.

The next part can be characterised by a new redistribution of hydraulic energy in the cut and the compensation of the values for tension components in the tangential direction to the formation of the surface and in the axial direction to the deepening of the cut with the creation of a so-called "belly" with rather low values of *RMS*, *Ra* until striations occur. These are a feature of the endurance fractures of metals and alloys, and thus the beginning of a zone of steady plasticity of deformation with a marked periodicity beginning to be formed. The striations usually form shapes of shallow, parallel rows. The

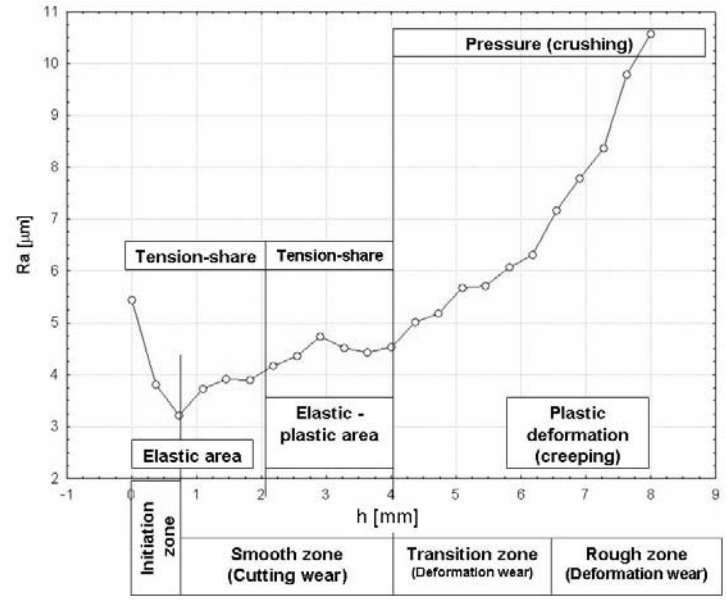

Fig. 10. *Dependence of the surface roughness, Ra, on the cut depth, h, geometrical and stress-deformation curve of topography zones*

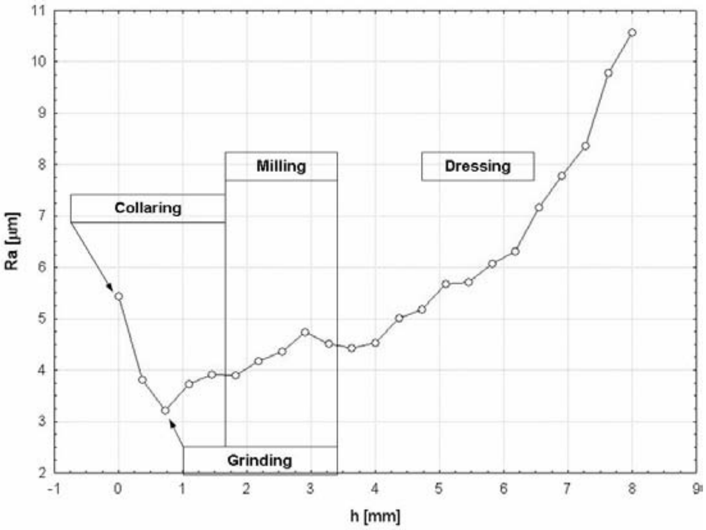

Fig. 11. *Dependence of the surface roughness Ra on the cut depth h and the expression of analogy concerning the proportions of the various technologies in the cut formation*

layout of the striations provides information about the local direction of the endurance fracture's propagation. From the standpoint of stress-deformation conditions, at the beginning the high stress and a rather smooth cut occur, and towards high values of *RMS*, *Ra* the stress diminishes proportionally to the increase in these values. We can say that the division of the cut into the initiation zone (h_I) can be used, which depends heavily on the material and, as for the technology parameters, especially on the selection of the traverse speed of the cutting head. Furthermore, a relatively smooth zone (h_{II}), where mainly a tension-shear combination prevails, can be determined, passing into the elastic-plastic area of the so-called transition zone (h_{III}). Another region with a prevailing pressure component is the so-called deformation zone (h_{IV}), as can be seen in Fig. 8. In terms of the consumption of strain energy, there are in principle three zones.

These zones are the initiation zone, characterised by the energy losses of the jet due to collaring the material, overcoming the elastic limit of the material and the energy stabilisation of the hydraulic and hydrodynamic conditions of the cut, the zone with a high proportion of strain energy in the creation of so-called smooth and transition zones, and a zone with a lower proportion, or shortage, of strain energy, which corresponds to the deformation zone. What is a specific feature of the surfaces generated by means of the AWJ is the fact that they are rough. Thus they may be regarded as surfaces produced by various classical technologies, such as collaring into the material in the initiation zone, grinding (high-energy area-zone) and machining in the medium part of the cut, across the area of rather rough turning, planing and rough dressing at the end of the cut (Fig. 11).

6 PROPOSAL FOR A DATABANK OF AWJ TECHNOLOGY CONTROL

The conceptual structure of the databank is characterized in Figure 12. The main input and output factors are sorted according to [6] so that a hydraulic factor, material factors, the shape and MESH of the abrasive, and the technical factors of the stream and hydro-devices create an output of energy characteristic of the stream. The material and dimensional properties of the samples depend on the energy load. Material parameters, like the tensile strength, the pressure, the torsion strength, the modulus of elastic compression, the weight, the Poisson number, the ultrasonic wave propagation speed, and the chemical composition, will represent, in addition to the main technology factor, the basic inputs.

The material constants determine the mechanical behaviour of the material and the character of induced power, the tension and the deformation field. The examination of a mathematical function between the input, i.e., the material and technology, and the output, i.e., the geometrical surface parameter, is the basis for their mutual influencing in the control system. The machining done by AWJ is a

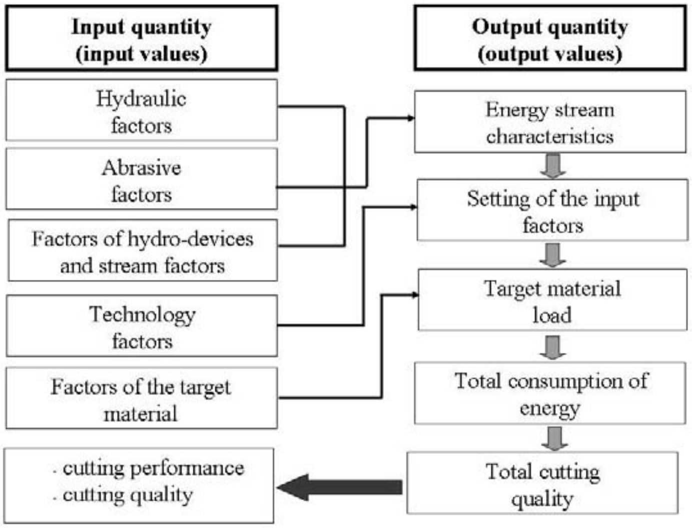

Fig. 12. *Conceptual structure of the databank*

process that is difficult in terms of technology. The project preparation, optimisation and the overall result of the AWJ machining are influenced by a number of factors. Partial influences of the factors are interconnected; some statistical-mathematical methods, such as factor analysis, which is presented, for example, in [7], have been applied to their optimisation and selection. Besides the cut surface topography parameters, the total energy consumption, the performance parameters and the manufacturing costs will be observed. The data will be systematically updated and statistically and analytically evaluated in order to be fully usable for the prediction of the geometrical surface condition and for the project of optimisation of the main AWJ process factors, which covers all kinds of materials used most frequently in technical professions.

7 CONCLUSIONS

An optical method was developed in order to characterize the basic geometrical properties of the topography of surfaces produced by the AWJ technology. On the basis of optical measurements the values of the *RMS* roughness in relation to the depth of cut *h,* can be evaluated. The main geometrical parameters of AWJ traces, such as the surface roughness *Ra*, the retardation Y_{ret} and the deviation of the cutting trace δ, were defined and determined. These are the properties that are considered to be very important for many reasons, known well in both theory and practice. This is especially the case for the surface roughness *Ra*. A databank for the systematic holding and processing of the measured data in relation to the technology and material parameters was drafted. In the framework of verification it was found that optical methods, with regard to many specific advantages over the classical surface measurements, also represent the substantial objectives of the output control in the AWJ technology. For the development of the theory and practice of AWJ technology, a basis was defined in the above-presented way for solving other complicated issues connected with the theoretical handling of the mechanism of interaction between the flexible cutting tool and the material, and with theoretical relations to the regime technology parameters of the process. From the evaluation of statistical and physical-analytical rules between the input and the output quantities, it is possible to proceed to the mathematical generalisation of these rules and the deducing of statistical and physical equations for predictive and design calculations of particular cuts. These calculations should form a theoretical basis for the selection of cutting parameters that are optimal for the given material as well as for the required parameters regarding the quality, performance and overall economics of machining works made with the AWJ stream.

ACKNOWLEDGEMENTS

The contribution was written thanks to support provided by the IGS-HGF VŠB TUO-2007-2103/516 grant project and the VEGA 1/1075/04, 1/4157/07, 2/5148/27 KONTAKT IČ ČR 119 and IČ SK 88, GA ČR 101/01/1104 and GA ČR 105/06/1516.

8 REFERENCES

[1] Bumbálek, B., Obvody, V., Ošťádal, B. (1989) Surface roughness. Praha, *SNTL* (in Czech).

[2] Brezina, I. (1991) Surface roughness. F*ine mechanics and optics*, No. 7, 1991 (in Czech).

[3] Hashish, M. (1984) Modeling study of metal cutting with abrasive waterjets. *Trans. of the ASME, Journal of Eng. Mat&Tech*, Vol. 106, No. 1, 1984.

[4] Hashish, M. (1989) Pressure effect in abrasive – waterjet (AWJ) machining. *Trans. of the ASME, Journal of Eng. Mat&Tech.*, Vol. 111, No. 7, 1989.

[5] Arola, D., Ramulu, M. (1997) Material removal in abrasive waterjet machining of metals, Surface integrity and texture. *Wear* 210, 1997.

[6] Guo, N. S. (1994) Schneidprozess und Schnittqualität beim Wasserabrasiusstrahl – schneiden. *VDI Verlag*.

[7] Hloch, S., Gombár M. (2006) Roughness of stainless steel surface in the process of cutting with abrasive waterjet. *MM Spectrum*. No. 7,8 (2006), pp. 48-50, ISSN 1212-2572 (in Slovak).

Authors' Addresses:

Dr. Jan Valíček
Prof. Dr. Vilém Mádr
Mining and Geological Faculty
VŠB-Technical University of Ostrava,
708 33 Ostrava, Czech Republic
valicek.jan@seznam.cz

Dr. Milan Držík
Institute of Construction and Architecture
Slovak Academy of Sciences
Dubravska 9
845 03 Bratislava, Slovak Republic
drzik@ilc.sk

Dr. Sergej Hloch
Dr. Agáta Radvanská,
Faculty of Manufacturing Technologies
Technical University of Košice
080 01 Prešov, Slovak Republic
hloch.sergej@fvt.sk
radvanska.agata@fvt.sk

Prof. Dr. Miloslav Ohlídal
Faculty of Mechanical Engineering
Brno University of Technology
Technická 2
616 96 Brno, Czech Republic
ohlidal@fme.vutbr.cz

Lupták Miloslav
Faculty of Metallurgy of Košice
042 00 Košice, Slovak Republic
milo.luptak@tuke.sk

Prejeto:
Received: 21.10.2006

Sprejeto:
Accepted: 21.2.2007

Odprto za diskusijo: 1 leto
Open for discussion: 1 year

Strojniški vestnik - Journal of Mechanical Engineering 53(2007)4, 233-240
UDK - UDC 629.1.015:[681.5:004.8]
Kratki znanstveni prispevek - Short scientific paper (1.03)

Uporaba logično mehkega krmiljenja za izboljšanje udobja vožnje vozil

The Use of Fuzzy-Logic Control to Improve the Ride Comfort of Vehicles

Yener Taskin - Yuksel Hacioglu - Nurkan Yagiz
(Istanbul University, Turkey)

V prispevku smo predstavili povsem novo metodo mehke logike krmiljenja aktivnega obešenja vozila. S to metodo izboljšamo udobje potnikov v vozilu brez izgube delovnega prostora pri ustavljanju. Kot vstopne veličine smo izbrali odvod navpičnega pomika vozila, upogib obešenja in sestavo teh veličin, kot izstopno veličino pa silo izvršilnika. S tako izbiro vstopnih veličin zmanjšamo zalogo pravil in skrajšamo čas, potreben za izračun. Predlagano krmiljenje smo uporabili na četrtinskem modelu vozila, pri ugotavljanju časovne odvisnosti smo, da bi bolje raziskali delovanje krmilja, upoštevali različne vozne razmere. Na koncu smo predstavili še frekvenčni odziv ter uspešnost predlaganega krmilja.

(Ključne besede: mehka logika, krmiljenje aktivnega obešenja, vplivi na udobje, delovni prostor)

In this study, a brand new fuzzy-logic method for the active suspension control of a vehicle is introduced. The method improves the ride comfort of passengers without losing any of the working space of the suspension. The derivative of the vehicle's vertical body displacement, the suspension deflection, and the combination of these variables were chosen as the inputs, and the actuator force was the output of the controller. This choice of input combination leads to a reduced rule base and a shorter computation time. The proposed controller is applied to a quarter-car model, and for the time responses different road conditions are considered in order to give a better understanding of the performance of the controller. Finally, the frequency responses are presented and the success of the proposed controller is discussed.

(Keywords: fuzzy logic, active suspension control, ride comfort, suspension working space)

0 INTRODUCTION

The main functions of vehicle suspensions are to suppress the vibration of the vehicle body and to achieve tire-road contact. Reducing the acceleration and displacement of the vehicle body provides the ride comfort for the passengers. Generally, vehicle suspensions are classified as passive, semi-active and active systems [1]. The term passive describes a suspension that is made up of the traditional suspension elements, i.e., a spring and damper. In passive suspensions the control objectives are obtained for limited frequencies and there is a conflict between the ride comfort, the road holding and the suspension deflection ([1] to [4]). Therefore, semi-active and active systems are receiving a great deal of interest in investigations to overcome these problems. Variable dampers or magneto-rheological (MR) dampers are used in semi-active suspension systems, whereas active suspensions include various actuators, like pneumatic, hydraulic, etc. In most of the studies these elements are used in parallel with passive elements to achieve the desired performance ([1], [2], [5] and [6]). In active suspension systems, controllers use the suspension working space by changing the original suspension length. Thus, in the controller design stage the suspension deflection should be taken into account; if not, the control action could cause the controllers to lock themselves and not to function properly, which leads to a harsh ride.

Different control methods are used in semi-active and active suspension systems. Fuzzy-logic control is one of the innovative control methods; it is based on the fuzzy-logic theory presented by Zadeh [7]. It is preferred because of its applicability to systems where the mathematical model is not known exactly and its ability to express the knowledge of experts in linguistic form ([8] and [9]). Much research has involved suspension control with fuzzy logic. Lee [10] presented a detailed survey of the fuzzy-logic controller in which a general methodology for constructing a fuzzy-logic controller and assessing its performance is described. D'Amato and Viassolo [11] proposed a controller including fuzzy logic to minimize vertical car-body acceleration and to avoid hitting the suspension's limits. Al-Holou *et al.* [12] combined the sliding-mode, fuzzy-logic, and neural-network control methodologies in order to enhance the ride and comfort. Huang and Lin [13] proposed an adaptive fuzzy sliding-mode controller to suppress the sprung-mass position oscillation due to road-surface variations. Guclu [14] presented a fuzzy-logic control for a vehicle without causing any degradation in the suspension's working limits. Kou and Li [15] proposed a GA-based Fuzzy PI/PD controller for a quarter-car active suspension system where the suspension deflection and its derivative are used as the inputs. Caponetto *et al*. [16] proposed a fuzzy-control approach to a sky-hook semi-active suspension system, where the fuzzy controller is optimized by means of a genetic algorithm. Sharkawy [17] proposed an adaptive fuzzy controller for a quarter-car active suspension system where the adaptive law is obtained using Lyapunov's direct method. An improvement in ride comfort and road handling with respect to LQR was shown via simulations. Rao and Prahlad [18] proposed a fuzzy-logic controller for a quarter-car model in which the inputs are the suspension deflection and its change, and the output is the change of the control signal. Yeh and Tsao [19] proposed a fuzzy-preview control scheme and a virtual damper concept to improve the performance while the vehicle is passing over a rough road.

The motivation for investigating vehicles' active suspension systems comes from the trade off between the control objectives of the suspension system. In this study a new fuzzy-logic approach is proposed in order to provide the suppression of vehicle-body bounce and acceleration while preserving the suspension's traveling limits. The controller is applied to a quarter-car model and numerical results are given to illustrate the performance of the proposed control strategy.

The rest of the paper is organized as follows. In Section 2, the vehicle model is presented. The proposed control method is explained in detail in Section 3. Next, the results of the application of the controller are given to reveal the success and the performance of the controller in Section 4. Finally, conclusions are drawn in the last section.

1 VEHICLE MODEL

Although passenger vehicles consist of four individual wheels, considering only one wheel is adequate when it comes to investigating the vertical dynamics and the main performance of an active suspension system as a quarter-car model, which is shown in Figure 1. In the diagram, m_1 and m_2 are the unsprung and sprung masses, respectively. The tire and suspension stiffnesses are denoted as k_1 and k_2. b_2 is the damping coefficient of the viscous damper and u corresponds to the control force that is produced by the actuator. y_0 is the road input to the tire. y_1 and y_2 are the absolute displacements of the unsprung and sprung masses, respectively. The suspension deflection is defined as $y_2 - y_1$. The pa-

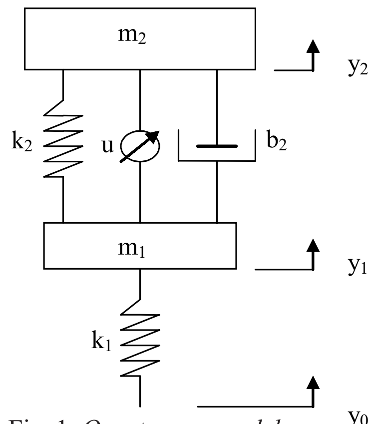

Fig. 1. *Quarter-car model*

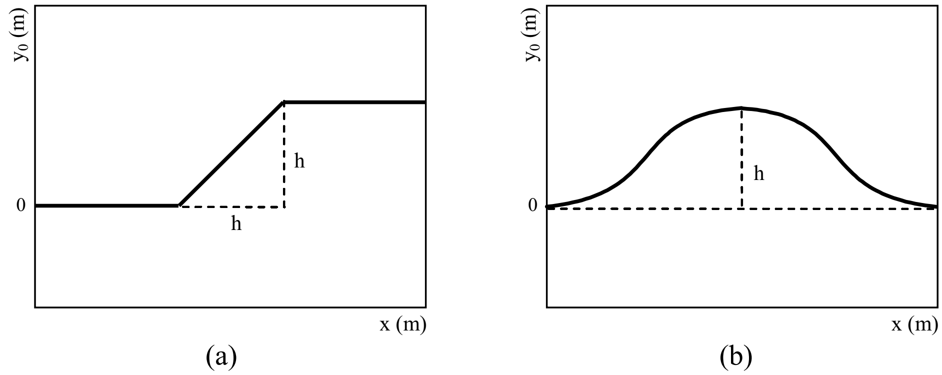

Fig. 2. *a) Limited-ramp road input b) Bump-road input*

rameters of the quarter-car model and the proposed controller are given in the Appendix.

The equations of motion for the quarter-car model are given below:

$$m_1\ddot{y}_1 + b_2(\dot{y}_1 - \dot{y}_2) + k_2(y_1 - y_2) + k_1(y_1 - y_0) = -u \quad (1)$$

$$m_2\ddot{y}_2 + b_2(\dot{y}_2 - \dot{y}_1) + k_2(y_2 - y_1) = u \quad (2).$$

In this study, the quarter-car model is subjected to the road inputs, as shown in Figure 2.a and 2.b. The vehicle model vibrates as it passes over the road profile with a constant velocity V during the first second of its travel. The bump-road equation [11] is:

$$y_0(t) = \begin{cases} h[1-\cos(8\pi t)]/2 & ; \quad 1 \le t \le 1.25 \\ 0 & ; \quad otherwise \end{cases} \quad (3).$$

2 CONTROLLER DESIGN

Fuzzy logic provides the ability to use the knowledge coming from experts, which is in linguistic form, according to fuzzy rules. Another property of fuzzy logic is its applicability to systems in which the exact mathematical model is not known. Because of these attractive features, it is used in a wide range of control applications.

There are three important steps in fuzzy-logic control: fuzzification, inference and defuzzification. In the first step the crisp variables are converted to fuzzy variables. In other words, membership functions are described for the input and output variables. In the second step the linguistic expressions are used to form the rules that constitute the rule base. In general, these rules are in the following form for a fuzzy controller with *n* inputs and a single output:

$$\text{IF } x_1 \text{ is } X_1 \text{ and } x_2 \text{ is } X_2 \text{ and } \ldots\ x_n \text{ is } X_n \text{ THEN } u \text{ is } U \quad (4).$$

Since the output values cannot be used directly, in the last step the fuzzy variables are converted to crisp values with an appropriate defuzzification method. In this study the centroid method, which is widely used in the literature, is used for the defuzzification of the fuzzy variables.

It is well known that conventional fuzzy-logic controllers operate like sliding-mode controllers with a boundary layer. It is thought that there exists a sliding line along the diagonal of the rule base and the control signal has opposite signs at the two sides. Therefore, evidence about the stability of the closed-loop control system can be obtained from an analogy between conventional fuzzy-logic control and sliding-mode control (Palm, [20]).

The aim of this study is to improve the ride comfort for passengers without causing any degradation in the suspension's working limits. Thus, a fuzzy-logic controller with three inputs and a single output is designed. The block diagram of the controller is given in Figure 3. The inputs are the derivative of the vehicle's vertical body displacement, $\dot{y}_{2N}$, the suspension deflection, $(y_2 - y_1)_N$, and a combination of these two inputs, $\lambda_N = \dot{y}_{2N} + \alpha(y_2 - y_1)_N$. Here, α is the weighting factor and the subscript *N* indicates that the variables are normalized.

Triangular membership functions are used for the fuzzy variables, as shown in Figure 4. NB, N, Z, P and PB denote negative big, negative, zero, positive, and positive big, respectively.

The input and output membership functions are defined on the [-1,1] closed interval, and the scaling factors (*SF*s) are used in order to map the crisp values to the corresponding fuzzy values. The relationships between the normalized and actual values

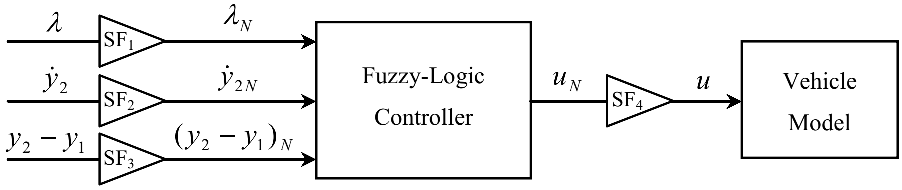

Fig. 3. *General structure of the control system*

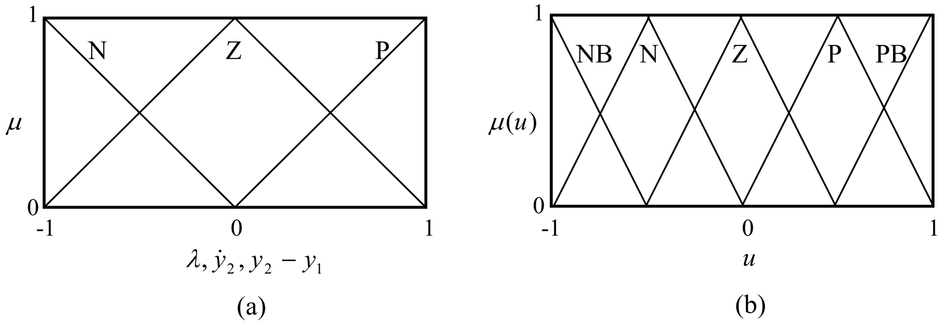

Fig. 4. *Membership functions a) input variables b) output variable*

are shown below.

$$\lambda_N = \lambda \, SF_1 \tag{5}$$

$$\dot{y}_{2N} = \dot{y}_2 \, SF_2 \tag{6}$$

$$(y_2 - y_1)_N = (y_2 - y_1) \, SF_3 \tag{7}$$

$$u = u_N \; SF_4 \tag{8}.$$

Since the aim of this study is to improve the ride comfort without causing any degeneration in the suspension's working limits, the input variable $\lambda_N = \dot{y}_{2N} + \alpha (y_2 - y_1)_N$ plays an important role in the construction of the rule base. Rendering this variable zero will fulfil the aim of the study. According to the sign of the input variables, there are six regions on the $(y_2 - y_1)_N$ vs. $\dot{y}_{2N}$ plane, as depicted in Figure 5.a. When λ_N takes negative values, that means either a negative suspension deflection exists or the suspension deflection tends to be negative because of the large vertical vehicle-body acceleration. Thus, during this time the control force should be positive, which pushes the vehicle body upwards. Similarly, for the positive values of λ_N, a negative force should be applied to the vehicle body. When λ_N assumes approximately zero values, which agrees with the design requirements, the control inputs are approximately zero. For the nonzero values of λ_N, the other two inputs of the fuzzy controller give information about the location of the system states. For example, if all the inputs are positive (1[st] region in Figure 5.a), i.e., a positive suspension deflection exists and the vehicle body is travelling upwards, then the control input is selected to be negative big. This choice of control input forces the vehicle body to travel downwards,

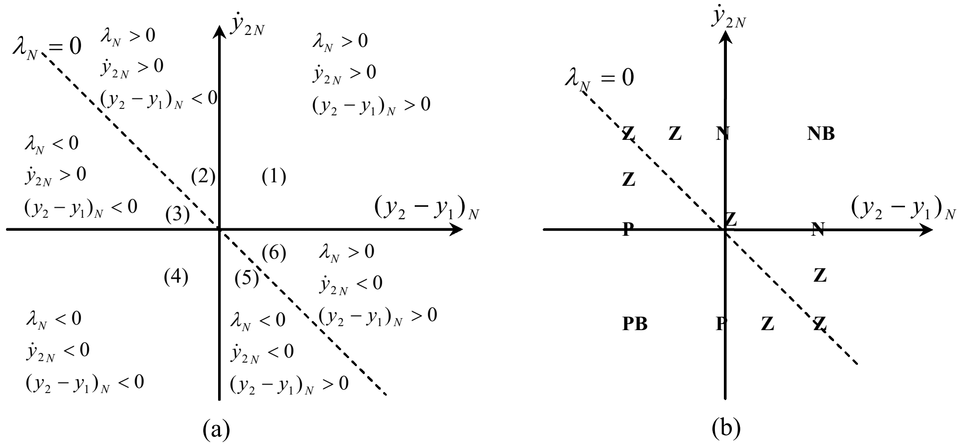

Fig. 5. *a) Evaluation of the sign of the input variables b) Graphical representation of the rules*

which results in zero suspension deflection and zero vertical velocity for the vehicle body. Suppose, however, that the suspension deflection is positive and the vehicle body is travelling downwards and the λ_N is negative (5th region in Figure 5.a), then the control input is selected to be zero since the internal dynamics of the system force the λ_N and the suspension deflection to be zero, spontaneously. The rule base is constructed in a similar way and given in Table 1.

A graphical representation of the rules is given in Figure 5.b. From this figure it is clear that the rules are arranged in such a manner that λ_N is rendered to be zero by applying certain control inputs. Next, the states are kept in the region where $\lambda_N = 0$ and the internal dynamics of the system render the suspension deflection and the vertical velocity of the vehicle body to be zero. Thus, all the states of the system are regulated to zero by the constructed rule base. In fact, it is possible to write 27 rules when three inputs are used. However, some of them are not physically realizable. For instance, if the suspension deflection and the derivative of the vertical body displacement are both negative, the first input variable, λ_N, cannot have a positive value. Thus, certain input combinations are not used during the construction of the rule table, which reduces the size of the rule base and decreases the computation time.

3 RESULTS

The controller is focused on the body bounce, the body acceleration and the suspension deflection. Thus, the controller is expected to improve the related control objectives. The improvements can be disclosed when the numerical results of the proposed controller are compared with the passive results.

In Figure 6.a, 6.b, and 6.c, the time responses are shown for a passive and an active suspension system, while the road input is a limited ramp. In Figure 6.a, for the passive suspension, the vertical movement of the vehicle body begins as the vehicle comes into contact with the obstacle and overshoots the height of the road profile. When the active suspension is considered for the proposed controller, the sprung mass softly settles on its steady value, as seen in the same figure. If the suspension deflection is also taken into account, it is clear that the suspension regains its original position, as seen in Figure 6.c. The suspension deflection reaches zero as the sprung mass settles. Thus, there is no permanent deflection in the suspension. The body acceleration is also decreased by the proposed control strategy, as shown in Figure 6.b.

In order to verify the performance of the proposed controller a typical bump-road input is also applied to the vehicle model and the time responses are given in Figure 7. It is clear that the magnitudes are reduced for the vertical body displacement and the vertical body acceleration, which indicates that ride comfort is improved greatly. It is also clear that the suspension working space is preserved for this road disturbance.

In Figure 8.a, and 8.b, the frequency responses for the vehicle body displacement and

Table 1. *Rule base for the control input u*

Input			**Output**
λ	$\dot{y}_2$	$y_2 - y_1$	u
P	P	P	NB
P	P	Z	N
P	P	N	Z
P	Z	P	N
P	N	P	Z
Z	P	N	Z
Z	Z	Z	Z
Z	N	P	Z
N	P	N	Z
N	Z	N	P
N	N	P	Z
N	N	Z	P
N	N	N	PB

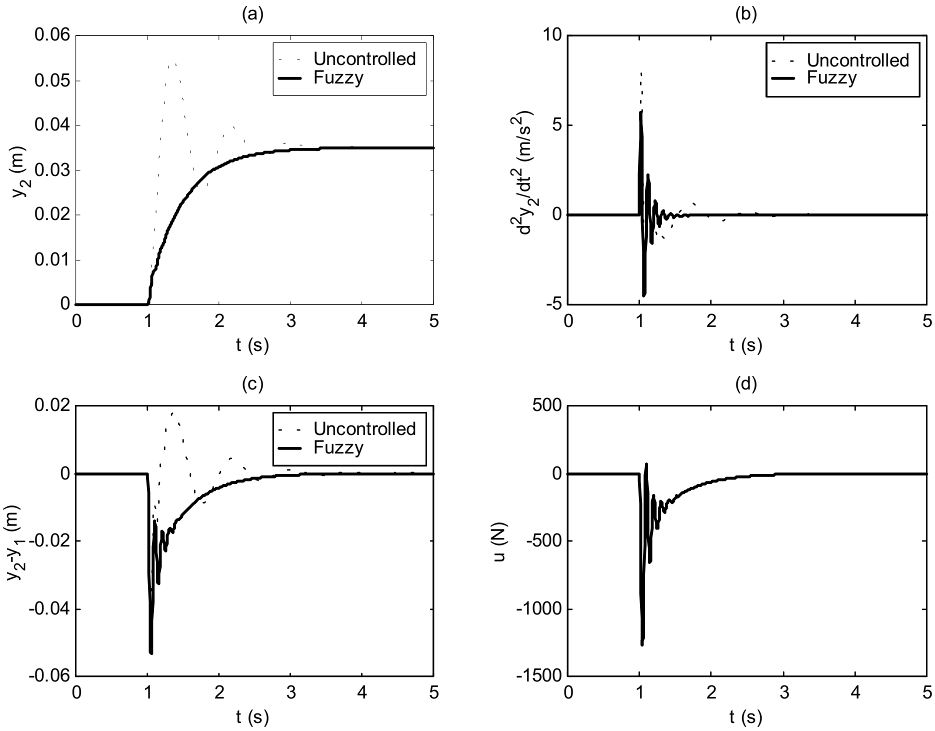

Fig. 6. *Time responses for the limited-ramp road input; a) Body bounce b) Body acceleration c) Suspension deflection d) Control force*

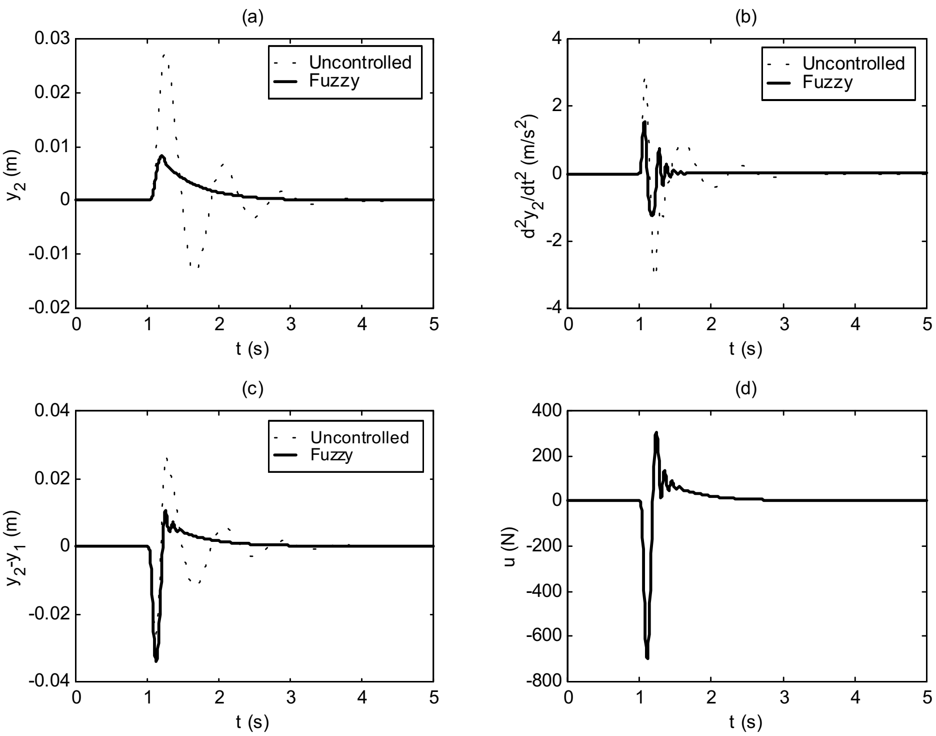

Fig. 7. *Time responses for the bump-road input; a) Body bounce b) Body acceleration c) Suspension deflection d) Control force*

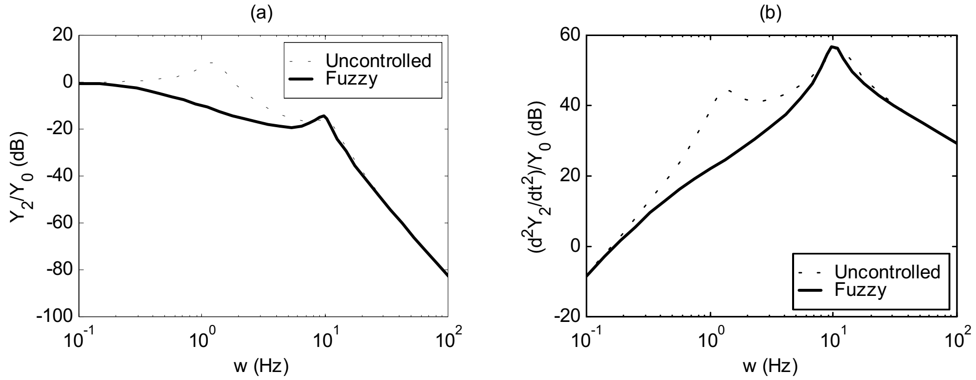

Fig. 8. *Frequency responses; a) Body bounce b) Body acceleration*

acceleration are shown for passive and active suspension systems. It is clear that the resonance frequency of the body on which the passengers are positioned is suppressed very well by the proposed controller around 1 Hz. The magnitudes are also reduced across a wide frequency range, which indicates that the ride comfort is improved.

To test the performance of the controller experimentally, an accelerometer will be used to sense the vertical motion of the vehicle body and LVDT sensors will be used to measure the suspension's working space. These data will be the inputs to microprocessors, which are programmed using the proposed fuzzy-logic control algorithm. Finally, the control inputs will be applied to the vehicle body using linear motors that will be used as actuators.

4 CONCLUSION

In this study a multiple-input, single-output fuzzy-logic controller is proposed in order to improve the ride comfort of passengers without causing any permanent reduction in the suspension's working space. The derivative of the vertical body displacement, the suspension deflection, and the combination of these two variables are used as inputs, and the controller force is the output. Although the fuzzy-logic controller has three inputs, only thirteen rules are required in order to fulfill the aim of the study. Time responses show that the vehicle body settles smoothly and that the suspension's working space is preserved. Finally, the frequency responses also showed that the ride comfort of the passengers was greatly improved.

5 APPENDIX

Numerical parameters of the quarter-car model
m_1 = 36 kg
m_2 = 240 kg
b_2 = 980 Ns/m
k_2 = 16000 N/m
k_1 = 160000 N/m
V = 72 km/h
h = 0.035 m

Numerical parameters of the proposed controller
SF1 = 1/0.3
SF3 = 1/0.1
α = 1
SF2 = 1/0.3
SF4 = 6000

6 REFERENCES

[1] Du, H., Sze, K. Y., Lam, J. (2005) Semi-active H_8 control of vehicle suspension with magneto-rheological dampers, *Journal of Sound and Vibration,* 283, (2005), pp. 981–996.

[2] Cherry, A. S., Jones, R. P. (1995) Fuzzy logic control of an automotive suspension system, *IEE Proc.-Control Theory Appl.,* 142(2), March 1995, pp. 149-160.

[3] Al-Holou, N., Weaver, J., Lahdhiri, T., Joo, D. S. (1999) Sliding mode-based fuzzy logic controller for a vehicle suspension system, *Proceedings of the American Control Conference*, San Diego, California, June 1999, pp. 4188-4192.

[4] Ramsbottom, M., Crolla, D. A., Plummer, A. R. (1999) Robust adaptive control of an active vehicle suspension system, *Proc Instn Mech Engrs*, Vol 213, Part D, 1999, pp. 1-17

[5] Yoshimura, T., Kume, A., Kurimoto, M., Hino, J. (2001) Construction of active suspension system of a quarter car model using the concept of sliding mode control, *Journal of Sound and Vibration,* 239 (2), (2001), pp. 187–199.

[6] Huang, S. J., Chao, H. C. (2000) Fuzzy logic controller for a vehicle active suspension system, *Proc Instn Mech Engrs*, Vol 214, Part D, 2000, pp. 1-12.

[7] Zadeh, L.A. (1965) Fuzzy sets, *Information and Control*, 8, pp. 338-353.

[8] Golob, M. (2001) Decomposed fuzzy proportional-integral-derivative controllers, *Applied Soft Computing*, 1, pp. 201-214.

[9] Liu, H., Nonami, K., Hagiwara, T. (2005) Semi-active fuzzy sliding mode control of full vehicle and suspensions, *Journal of Vibration and Control*, 11 (8), pp. 1025-1042.

[10] Lee, C. C. (1990) Fuzzy logic in control systems: Fuzzy logic controller-Part I and Part II, *IEEE Transactions On Systems, Man, and Cybernetics*, Vol. 20, No. 2, March/April 1990, pp. 404-435.

[11] D'Amato, F. J., Viassolo, D. E. (2000) Fuzzy control for active suspensions, *Mechatronics*, 10, 2000, pp. 897-920.

[12] Al-Holou, N., Lahdhiri, T., Joo, D. S., Weaver, J., Al-Abbas, F. (2002) Sliding mode neural network inference fuzzy logic control for active suspension systems, *IEEE Transactions On Fuzzy Systems*, Vol. 10, No. 2, April 2002, pp. 234-246.

[13] Huang, S. J., Lin, W. C. (2003) Adaptive fuzzy controller with sliding surface for vehicle suspension control, *IEEE Transactions On Fuzzy Systems*, Vol. 11, No. 4, August 2003, pp. 550-559.

[14] Guclu, R. (2004) The fuzzy-logic control of active suspensions without suspension-gap degeneration, *Strojniški vestnik*, 10 (2004), pp. 462-468.

[15] Kuo, Y.P., Li, T.H.S. (1999) GA-based fuzzy PI/PD controller for automotive active suspension system, *Transactions on Industrial Electronics*, 46(6), pp. 1051-1056.

[16] Caponetto, R., Diamante, O., Fargione, G., Risitano, A., Tringali, D. (2003) A soft computing approach to fuzzy sky-hook control of semiactive suspension, *IEEE Transactions on Control Systems Technology*, 11(6), pp. 786-798.

[17] Sharkawy, A.B. (2005) Fuzzy and adaptive fuzzy control for the automobile's active suspension system, *Vehicle System Dynamics*, 43 (11), pp. 795-806.

[18] Rao, M.V.C., Prahlad, V. (1997) A tunable fuzzy logic controller for vehicle-active suspension systems, *Fuzzy Sets and Systems*, 85, pp. 11-21.

[19] Yeh, E.C., Tsao, Y.J. (1994) A fuzzy preview control scheme of active suspension for rough road, *International Journal of Vehicle Design*, 15, pp. 166-180.

[20] Palm, R. (1992) Sliding mode fuzzy control, in *Proceedings of the IEEE International Conference on Fuzzy Systems*, San Diego, CA, pp. 519-526.

Authors' Address:
Yener Taskin
Yuksel Hacioglu
Nurkan Yagiz
Department of Mechanical Engineering
Faculty of Engineering
Istanbul University
34320 Avcilar, Istanbul, Turkey
ytaskin@istanbul.edu.tr
yukselh@istanbul.edu.tr
nurkany@istanbul.edu.tr

Prejeto: Received: 5.6.2006
Sprejeto: Accepted: 25.10.2006
Odprto za diskusijo: 1 leto
Open for discussion: 1 year

Strojniški vestnik - Journal of Mechanical Engineering 53(2007)4, 241-252
UDK - UDC 007.52.001.63:519.876.5
Kratki znanstveni prispevek - Short scientific paper (1.03)

Funcijsko usmerjeni teoretični okvir za načrtovanje mehatronskih sistemov

A Function-Oriented Theoretical Framework for Mechatronic System Design

Xu Yong - Zou Huijun
(Shanghai Jiatong University, China)

Predstavljena je nova funkcijsko usmerjena teoretična mreža za razvoj metod načrtovanja mehatronskih sistemov. Vključili smo tehnološko neodvisni delovni opis vidikov mehatronskega sistema, kot so 1) povezave in razlike ciljne funkcije, spreminjevalne funkcije in prehoda stanja, 2) sestava obdelave podatkov in 3) drugotne funkcije. Vse razprave smo nato povzeli v zbirki aksiomov, ki tako oblikujejo modele načrtovanja in metode za mehatronske sisteme.

(Ključne besede: mehatronika, delovne usmeritve, ciljne funkcije, obdelava podatkov)

A new function-oriented theoretical framework for the development of mechatronic system design methods is presented. We include a technology-independent functional description of aspects of a mechatronic system, such as 1) the relations and distinctions among the purpose function, the transformation function and the state transition, 2) the structure of the information processing and 3) the secondary functions. All the discussions are then summarized in a set of axioms, which then form the basis for devising design models and methods for mechatronic systems.

(Keywords: mechatronics, function oriented design, purpose functions, information processing)

0 INTRODUCTION

Mechatronic technologies combine mechanics with electronics and information technology (mostly software technology) to form both a functional interaction and a spatial integration in components, subsystems and systems. Only by treating mechatronics as an independent engineering discipline, instead of just a combination of traditional engineering fields, is it possible to exploit the full potential of the symbiosis of mechanics, electronics and software.

Contributions to a general product theory can be found in cybernetics, system theory, and system engineering ([1] to [3]). In addition, a large amount of published literature ([4] to [9]) has investigated definitions and representations for the function and the functional property of technical systems/products. Unfortunately, few of them show sufficient or substantial focus on mechatronic systems due to an inadequate discernment of the functional nature and the characteristics of mechatronic systems. As a result, there are few discussions concerning the correlations among the transformation functions, the purpose functions and the state transitions relating to mechatronic systems.

The purpose of any technical system is to support a transformation or process. The effects necessary for the transformation of a process object (material, energy, data, or biological object) are delivered in an interplay between the system and the human operator. The function of a technical system is, therefore, usually described as a continuous flow of material, energy and information. However, a mechatronic system works in different states, and the function of the mechatronic system depends on its states. So the description of the continuous function transformation must be supplemented by a model explicitly describing the states of the system and the transitions between the states.

The design methodology that handles all the aspects of the mechanics/electronics/software combination is still missing because there are significant differences between the designing mechanics, the electronics and the software. Not only are different technical skills required, but the very nature of the design problems differs in terms of the functions to be realized, the types of solutions available, and the realization of the intended functions.

A major difficulty is that the term 'function' is understood and described very differently, ranging from physical effects and the transformations of material/energy/information, to logical relations between the data operations. This means that it is difficult to come to a holistic, abstract understanding of a mechatronic system, i.e., to describe a function structure. The chief obstacle to creating a holistic function structure for a mechatronic system is the absence of traditional methods and languages (such as those describing 'pure mechanics') in the description of the logical relations between functions.

The different design characteristics of mechanics, electronics and software indicate that a new function-oriented theoretical framework for the development of mechatronic system design methods is one of the most important research areas. This paper concentrates on the aspects of a technology-independent functional description of mechatronic systems in the conceptual design phase, where mechatronics is most clearly distinguishable from the traditional technologies of which it is comprised.

All the discussions are summarized in a set of axioms expressing the fundamental characteristics or relations between the characteristics of mechatronic systems, and those most important principles directly applicable to mechatronic systems design, which consequently form the basis for devising design models and methods for mechatronic systems.

1 A FUNCTION-ORIENTED THEORETICAL STARTING POINT FOR MECHATRONIC SYSTEM DESIGN

1.1 The mechatronic system in relation to a general design procedure

It is claimed in this paper that product (technical system) design involves successively establishing four systems, each corresponding to a (mental) working domain for the designer, as shown in Figure 1. These four systems represent four different aspects of the product:

1) The transformation function (or process) system: a structure of processes, where the focus is on the purpose-oriented transformation of process objects like material, energy and information.
2) The (purpose) function system: a structure of purpose functions or effects needed in the product to create the specified transformations. An effect is a physical effect. For example, the interaction between the teeth of two gear wheels constitutes a gear as a component, and the physical effect of a gear is the transfer of rotational speed and torque.
3) The component (or function carrier) system: a structure of components. A component in the paper can be understood as a category of physical entities that creates the required physical effects and exhibits similar working principles to realize a required (purpose) function. The mode of action of a component is based upon a physical effect. Some components are in direct physical contact with the process object, while others deliver effects in the vertical chain of causality [8].
4) The parts system: a structure of single product parts, where the focus is on the allocation or distribution of the components into parts, which can be produced and assembled so that every machine part contributes to the totality.

This then leads to:

- The transformation function (or process) of a mechatronic system/product is the action that changes a process object (material, energy or information) from an input state to a desired output state. An example of the process in a mechatronic system can be identified in an electronic photocopier: 'The line pattern on the original paper is read, and a similar pattern is printed on copy paper'.
- The purpose function is the ability of the mechatronic system to create an expedient effect needed to realize a desired transformation, and the sum of all the necessary effects constitutes the purpose of the system. A mechatronic system is an effect structure with a causality relationship of the 'if…then…' type between the purpose functions and the effects of the system.

The process of product/system design cannot be described as a simple sequence of activities belonging to each domain. The human designer has the ability to freely jump back and forth between the

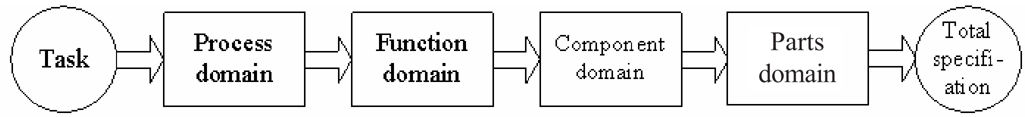

Fig.1. *A general procedure for technical system/product design*

four different perceptions of the product in his/her mind in an iterative sequence.

The main advantage of the general procedure is that it allows a precise positioning of design models and design methods, either within a particular domain or on a transition from one domain to another. In other words, knowledge of the domains in product design permits designers to develop design methods attached to one domain or to the transition from one domain to another. Using a catalogue of electronic components, for example, is a method for proceeding from an abstract description of a function to a physical realization.

The purpose of a mechatronic system is to facilitate a technical process, i.e., to effect the transformation of a process object from a given state to a desired state. The mechatronic system is not in itself a technical process; instead, it exerts the effects necessary to make the technical process happen. (For most technical processes, the effects created by the system in collaboration with a human operator can be understood as purpose functions). A mechatronic system can accordingly be regarded as a system of transformation functions, of purpose functions, of components, of parts.

Since the function of a mechatronic system depends on the state of the system, it is believed that mechatronic system design can be based directly on the general design procedure above, provided it is extended to deal with the logical concept of state transitions.

1.2 The function characteristics of mechanics, electronics and software

The term 'function' is used in mechanics, electronics and software. In machine-design theories it is common to describe the main purpose of a machine in terms of the transformations of material, energy and information. However, when adopting the term 'functions', designers think not only of transformations, but also of the 'effect needed in a machine' or purpose functions. Indeed, there seems to be a duality between transformation functions and purpose functions.

In a mechanical system information cannot exist independently; it must be attached to the substance of either a material (a punched card carries information) or an energy (hydraulic pressure may carry information). In machine design, the handling of energy and material is emphasized in comparison with information aspects.

In electronics design, function may be completely described as the transformations of electric properties (voltage, current, frequency, etc). In principle, some are transformations of information attached to energy, but the circuit designer usually ignores the energy aspects and only regards the flow of signals. Later, energy aspects always pop up as a recurring nuisance: heat dissipation, non-ignorable resistance in conductors, emitted electrical noises, etc.

In software design, the abstract function of a program can be described as transformations of data and logical relations of the 'if …then…' type between transformations. At each level of the program it is possible to distinguish between the data to be transformed and the control data. In software, data (information) can be handled independently of energy representation, even though it will be tied to the electrical properties, once the program is implemented in the electronics hardware.

2 THE FUNCTION-ORIENTED THEORETICAL FRAMEWORK FOR MECHATRONIC SYSTEM DESIGN

The interior structure of a mechatronic system, independent of any technology realization, is explained in this section. The most important issues about the functions of a mechatronic system are the applicability of the purpose function concept in a mechatronic system, the role of state transitions in a functional framework and the structure of information processing in the mechatronic system.

2.1 The function structure of mechatronic system

The completeness conditions of the function structure of a mechatronic system must be expounded from three views, i.e., the transformation function, the purpose function and the state transition.

2.1.1 The transformation function and the purpose function

(1) The transformation function and the purpose function

Accordingly, the mechatronic system can be regarded as the structure of the transformation functions or the structure of the purpose functions with causal or logical relations. The link between the transformation function and the purpose function is the choice of technology. (Here, 'technology' must be understood as the kind and sequence of the subprocesses of a process and the interaction in space and time between the process objects and the effects, which create the transformations) [9]. This means that the designer has to decide on a general technology before he/she can transform a process structure into a structure of purpose functions.

The concept of the purpose function is important, because it explains the step between the description of the transformations and the actual realization of functions through the physical principles in the system, i.e., the components. Also, the term comes close to the designer's practical understanding of system functions. For instance, the function of a ball bearing or of a static structure is much more easily explained in terms of effects than in terms of transformations.

A discussion of a transformational versus a purpose functional description of a mechatronic system really comes down to whether the machine itself is transforming the process object involved, or whether it is merely providing the effects necessary to facilitate the main transformation, which is then realized somehow externally to the machine. The purpose relates to the effect that the component provides to a system at a higher level. The transformation relates to the object (material, energy) that is processed by the component itself.

The concept of purpose functions was derived from observing a material-transforming machine, because there the distinction between transformation function and purpose function is evident. The effects created by the machine can be described almost independently of the transformation taking place.

One example is the fully automatic ECG (electrocardiogram) electrode manufacturing machine illustrated in Figure 2. A basic layer of foam is cut, a label is attached, and then a rivet, a ring and a foam block are added and so on, all in a sequential pattern. The effects of the machine corresponding to those processes are to provide a cutting effect and to generate a circular pattern, to establish the position and provide an attachment force for the label, etc.

The relations shown in the figure between purpose functions are of the causal type: all the purpose functions are necessary to accomplish the required transformation.

Is a purpose functional description of computer programs possible? In fact the definition of the purpose function rules out this option. Software cannot in itself exert any effect on a technical process – only the combination of computer software and hardware can do that. The functional descrip-

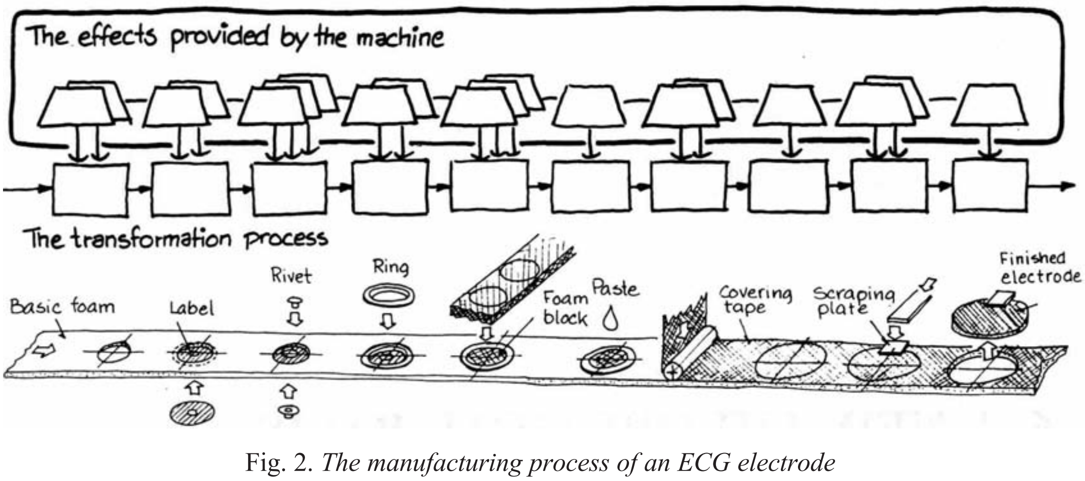

Fig. 2. *The manufacturing process of an ECG electrode*

tion of software is limited to the process domain, i.e., data transformation and state-transition modeling.

For energy-transforming machines the distinction between the transformation function and the purpose function is not so evident. A mechanical gear, for instance, transforms the rotary energy from one speed of revolution to another. Here, it becomes difficult to point out effects that the machine exerts to facilitate the transformation.

Energy transforming processes are central to any mechatronic system, because information is mostly tied to energy. Electronic circuits, for instance, realize only energy transformations, i.e., those of electronic signals. The interpretation of purpose functions in energy-transforming systems must therefore be examined more closely.

(2) The representations of the transformation function and the purpose function

A reasoning based on the analysis of well-known systems is necessary, i.e., one must ask which functions that existing systems and components fulfill are expressed in terms of transformations and exerted effects. From such reasoning it may be possible to generalize findings that are also applicable to the synthesis of non-existing systems.

It is presented as an axiom in the paper that transformation functions (or processes) and purpose functions can be distinguished by the strictly verbal formulation of verb/noun combinations.

The transformation function can be expressed in passive constructions of the form:

{object (noun)} is {transformed (verb)}

For instance, for a turntable: 'record is rotated', the state of the object 'record' is changed from non-rotating (input) to rotating (output) in the process.

The purpose function can be expressed actively to denote the purpose of the machine:

to {activate (verb)} {effect (noun)}

For instance, for rotating the record in the above example, the purpose function of the turntable is 'to create rotation', since 'rotation' is the effect exerted by the machine. The following table lists some examples:

It is evident from the list that the same component may serve several different purpose functions, depending on the system it is part of. The purpose of the gear, for instance, could also be 'to ensure sufficient torque' or 'to ensure correct orientation of movement'.

When observing the purpose function and the transformation function of individual components, functions seem to be formulated on different levels. The purpose relates to the effect that the component provides to a system at a higher level, but the transformation relates to the object (material, energy), which is processed by the component itself. The purpose of the motor, for instance, is 'to create rotation' in order to facilitate a transformation of some objects in a system, where the motor is a component. If we ask, 'How does the motor create rotation?', then the answer is, 'By performing the transformation of electrical energy into rotational energy'. This transformation process is only one of a number of alternative ways to 'create rotation', another is, 'By performing the transformation of potential energy into rotational energy' (e.g., a spring).

So it can be concluded as an axiom that there is a causal hierarchical relationship between the purpose functions and the transformation functions. A transformation requires different effects (the purpose functions) from the system, and an effect can be realized by alternative transformation functions on a secondary level.

Table 1. *Components with associated transformation functions and purpose functions*

Component	Transformation function	Purpose function
Motor	Electric energy is transformed into rotation	To create rotation
Gear	Rotation energy is transformed into revolution/torque	To ensure suitable revolution or torque
Electronic amplifier	Signal is amplified	To ensure sufficient amplitude
Battery	Energy is stored	To provide power
Diode	AC signal is rectified	To reject signals of negative polarization

Typical electronic (energy transforming) components can also be described in terms of purpose functions. Such a description is not common for electrical engineers and will even appear alien to them, but the purpose-function concept can help to clarify the hierarchical pattern of functions and alternative sub-solutions in electronics design.

2.1.2 The state transition and the transformation function

Two types of transformation functions can be distinguished: continuous and multi-state types. The multi-state type is characterized by its external control input.

In the continuous type of function-transformation process a function is described as a continuous flow of material, energy and information, and the output has a 'continuous' quality, i.e., it depends only on the state of the input (e.g., conducting, amplifying, transducing). However, when describing a complete structure of 'continuous' transformation functions, the different states of the system cannot be expressed explicitly. So a full functional description of a mechatronic system cannot be accomplished by using transformation functions only.

The mechatronic system works in different states (as a minimum there are the on and off states), and the function of a mechatronic system depends on the states of the system. Transitions between states are controlled by logical conditions (e.g., if a switch is turned on by the operator, then the machine changes to its on state). Nevertheless, when modeling the state-transition behavior, the flow of information is not clear – information is required for a change of state. This implies that the functions of mechatronic systems likewise cannot be described properly by state-transition presentations only.

This conflict between the continuous function transformation and the state-transition process is a primary obstacle to mechatronic design, since mechanical and electronics engineers have an ingrained mode of functionally oriented thinking, whereas software designers are preoccupied with sequences of operations and causal relations. So the description of the continuous function transformation must be supplemented by a model explicitly describing the states of the system and the transitions between states (e.g., a Petri-net). In fact, a transformation function belonging to the function structure of a mechatronic system must be considered to be of the multi-state type if it causes the system output to change state momentarily due to an external logical input. Moreover, a structure of transformation functions has multiple states, if at least one of its elements is of the multi-state type.

It should be noted that the type, i.e., continuous or multi-state, of the function-transformation structure is related to different scopes of observation. A subsystem with multiple states may be regarded as a one-state, i.e., continuous, system on the next higher level if the external input causing the change of state becomes internal. For example, the function of a switch has two states (on/off), but if the switch forms part of a pulsing relay, the function becomes continuous, as shown in Figure 3. It is rather a question of the scope of the observation in the hierarchical structure of systems and subsystems.

Then, how to single out the logical functions (logical functions are closely related to the understanding of the state transitions of mechatronic systems) of a multi-state transformation function system? The multi-state function substituting principle is presented as a theorem for the problem: if a multi-state function is present in a transformation-function structure, then it is possible to substitute this function by a state-transition structure and a continuous-transformation structure for each state of the system. It is the case, therefore, that each state of a mechatronic system defines one particular structure of continuous transformation functions.

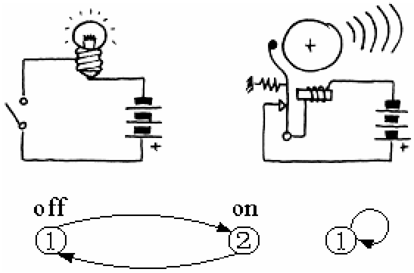

Fig.3. *The function of an electric switch: a one- and a two-state system*

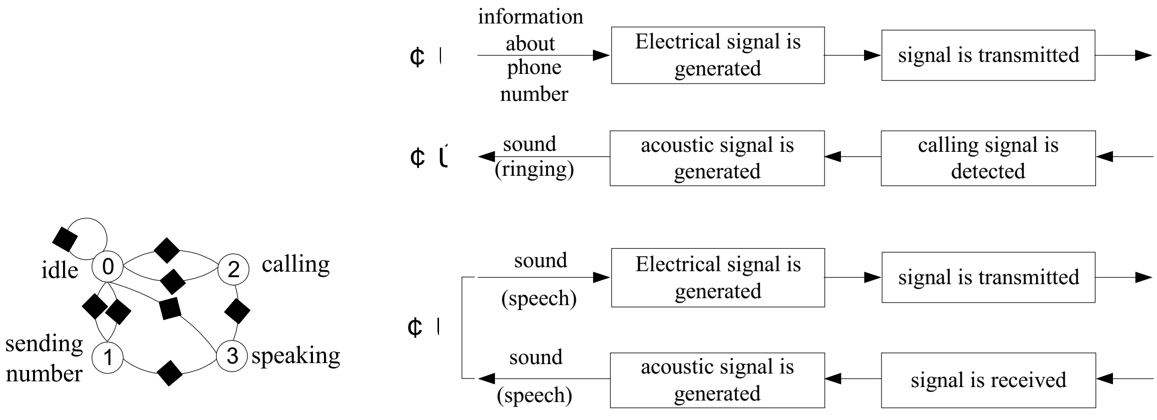

State transitions Transformation-function structure

Fig.4. *The transformation functions and state transition of a telephone*

The example of a telephone system can be used to illustrate the above discussion. In order to transmit spoken messages rapidly over a distance, the acoustic signal cannot be transmitted directly, but must be transformed into an electrical signal before it is returned to an acoustic signal again after being received by the other side. The principal functions of a telephone system are just the sound-electricity and electricity-sound signal transformations.

As shown in Figure 4, a telephone can be modeled in the process domain (transformation-function structure and the state/transition diagram) and in the function domain (purpose-function structure). The telephone has four states, of which one is idle.

If the function of the system is described in terms of the transformation only, then the output object of one or more blackboxes will exhibit three working states (sending number, calling and speaking). Instead, a 'continuous' transformation structure can be established for each working state of the system, and the structure of the states and transitions can be described separately.

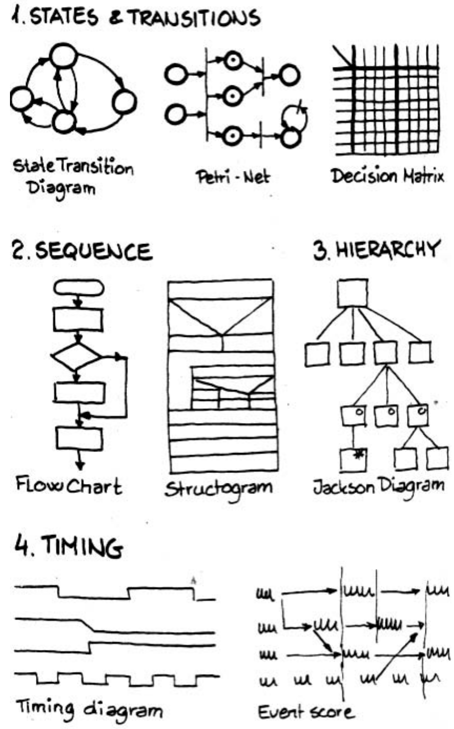

Fig.5. *The logical dependencies between the transformation functions of a system*

In other words, it is suggested that the transformation-function structure and the state-transition structure of a mechatronic system complement each other and therefore should be described separately. The logical dependencies between sub-processes can be expressed in a number of different model types, according to different foci. Figure 5 offers some examples, illustrating the following four aspects:

(1) States and transitions, focusing on the states of the system and the conditions for changing from one state to another. Typical model types: state/transition diagram, Petri net.
(2) Sequential procedure, where the one-by-one execution of sub-processes is emphasized: Flow chart, structogram.
(3) Hierarchical pattern, where the structure of subordinate levels of the processes is important: Jackson diagram.
(4) Timing conditions, where the timing of parallel transformations is critical: Timing diagram, event score.

2.1.3 The state transition and the purpose function

The function structure can be regarded as a table of contents of the necessary effects (observed on the hierarchical level) in the paper. Therefore, if the system has multiple states, each state of the system requires a different set of effects in the total structure of the purpose functions. Figure 6 shows the purpose-function structure of the previous example of a telephone system. Each of the four states of the system requires a set of purpose functions.

It is only possible to illustrate the logical relations between functions by connecting lines, to a certain extent. We believe that the main advantage of the purpose-function structure is the total view of the necessary effects in the system. Therefore, it provides a good starting point for allocating technology, i.e., for suggesting solutions in the physical entity domain.

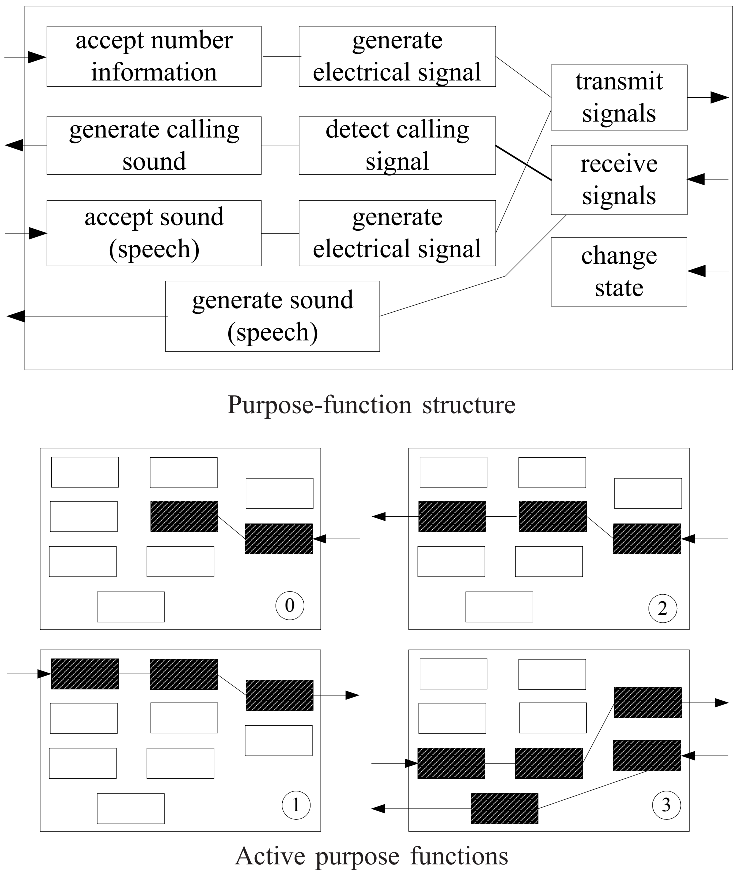

Fig.6. *The functions of a telephone*

2.2 The structure of information processes

Information is produced both by and for people. Both the data and the messages exchanged between people are subsets of information. The meaning of the information adopted here is rather cybernetic, i.e., the information is an independent category of transformation objects in addition to material and energy.

The transformation of information (signal processing) is the dominant form in a mechatronic system, either as the primary function or as the control function (a logical function is a discrete type of control function and basically deals with the semantic value of the information in order to derive decisions) of material or energy transformations. Control functions constitute the logical relations between the purpose functions of the mechatronic systems.

A mechatronic system basically handles two types of information:

- Process information, which is transformed, i.e., processed, by the system regardless of its semantic value.
- Control information, which is applied by the system for control purposes (the control of energy or material transforming processes), i.e., it is 'understood' by the system.

It is justified that both the process information and the control information of mechatronic systems have relative meanings at different hierarchical levels. An electronic feedback loop in a robot, for instance, clearly carries control information, since the purpose of the arrangement is to control the movements of the system. When observing the feedback sensor and the signal-conditioning circuits locally, however, the type of information treated has a process character. As far as the sensor and preamplifiers are concerned, the semantic value of the process information has no influence on their functions.

We believe that the process and control information in a mechatronic system in general appear alternately in a hierarchical structure: control information needs processing functions and processing functions are likely to be governed by control information on the next lower level (for example, information from an image sensor must be processed before controlling the robot programs on the next level), see Figure 7. In the figure, number "4" and "2" denote the control information, and number "3" and "1" denote the process information.

2.3 The secondary functions of a mechatronic system

Although the topic of this paper is just technology-independent functional descriptions, in order to ensure theoretical completeness and consistency, secondary functions (including the control function) of mechatronic systems will still be briefly discussed in the following.

In general, any primary function of a mechatronic system will need the simultaneous realization of some, but not necessarily all, secondary functions. An appropriate set of secondary functions includes: the power function, the control function, the interface function, the protection function, the communication function and the structure function.

Of these, the control function governs the state of the means realizing a primary function and the functional performance in accordance with external inputs, e.g., a feedback loop. The control function occupies a special position in mechatronic systems, since it is often realized by a multifunctional microprocessor with software. Two important statements can be derived from existing design theories (especially from those of machine design):

- The control function is a secondary function and always depends on the choice of means to realize a primary function.

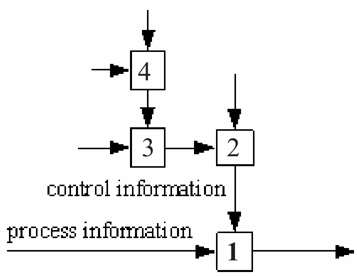

Fig. 7. *The process/control information hierarchy in mechatronic systems*

- The control function belongs to different levels of the function/means hierarchy.

In other words, it does not make sense to discuss the control function until the means to realize the function to be controlled has been decided on. And the interrelations between different control tasks in the system quickly become complex, because they connect controls on different hierarchical levels.

Both working functions and control functions in a mechatronic system can, at least theoretically, be realized in any or alternative combinations of mechanical, electronic and information technologies and furthermore performed by the operator of the mechatronic system. The state transition behavior of a mechatronic system is determined by the structure of the control components and their programmable instructions. Control components realize the logical relations between purpose functions on the same and different levels of the causal chain of functions and means.

The aspect of recursiveness is important: the secondary functions can themselves be regarded as primary functions on the next lower level of the hierarchy, each requiring some new secondary functions. This means realizing the function, which determines which types of secondary functions are needed on the next level. So the power function of a higher level may mean, for instance, the need for a control function, which again may require power.

3 CONCLUSIONS

There is a growing understanding that high-quality products can best be achieved through the use of methodical procedures. A comparison of the deign characteristics of mechanics, electronics and software, indicates that the most important areas for mechatronics research are a theoretical framework for the functional understanding of mechatronic systems, and design models (a ‘common language’) to describe the functional structures and the design concepts for such systems. In particular, the early stage of mechatronic-system design is in need of a methodology for functional description, conceptual design, etc. Accordingly, the functional basis, i.e., the functional principles for mechatronic system design, is the main topic of this paper.

It is advantageous to acquire a general theory from machine-design literature and models for handling the sequence and state transitions from software literature, in order to form a mechatronic system theory. It is also true that a synthesis theory for mechatronic systems can be based directly on the general design procedure, provided it is extended to deal with the logical concept of state transitions.

A new function-oriented theoretical framework for mechatronic system design is formulated in a set of axioms expressing the fundamental characteristics or relations between the characteristics of mechatronic systems, and essential conditions for the structured understanding of mechatronic systems, which consequently form the basis for devising design models and methods for mechatronic systems.

This research marks a new attempt to describe a function-oriented theoretical framework for mechatronic design. It is based on, if possible, a complete knowledge of product development practice in industry. The proposed theory permits the explanation of a great many observed phenomena in the literature and in industry, and it covers the common functional basis of system models and design principles.

4 APPENDIX: AXIOMS OF MECHATRONIC SYSTEM THEORY

Axiom 1: A mechatronic system can be regarded as a system of transformation functions, of purpose functions, of components, and of parts.

Axiom 2: Transformation functions (or processes) and purpose functions can be distinguished by a strictly verbal formulation of verb/noun combinations.

Axiom 3: There is a causal hierarchical relationship between purpose functions and transformation functions. A transformation requires different effects (purpose functions) from the system, and an effect can be realized by alternative transformation functions on a secondary level.

Axiom 4: The mechatronic system works in different states (at least in an on- and an off- state), and the function of a mechatronic system depends on the states of the system.

Axiom 5: The transition from one state to another is caused by logical inputs that are external to the mechatronic system.

Axiom 6: A subsystem with multiple states may be regarded as a one-state (continuous) system on a next higher level, if the external input causing the change of state has become internal.

Axiom 7: Two types of transformation functions can be distinguished: continuous and multi-state types. The multi-state type is characterized by its external control input.

Axiom 8: A structure of transformation functions has multiple states, if at least one of its elements is of multi-state type.

Axiom 9: Each state of a mechatronic system defines one particular structure of (continuous) transformation functions.

Axiom 10: Each state of a system requires a different set of effects in the total structure of purpose functions.

Axiom 11: A mechatronic system handles two kinds of information:

- 1 process information, which is treated regardless of its semantic value;
- 2 control information, which is directly applied ('understood') by the system.

Axiom 12: Control functions constitute the logical relations between the purpose functions of the mechatronic system.

Axiom 13: Control functions are secondary functions, which always depend on the choice of the means to realize a primary function.

Axiom 14: Both working functions and control functions in a mechatronic system can be realized in alternative combinations of mechanical, electronic and information technologies.

Axiom 15: There is a causal relationship between purpose functions and components: A function can be realized by alternative components, and each component will in turn require purpose functions on a secondary level.

Axiom 16: For the realization of any function, some or all of the following set of secondary functions are simultaneously required: the power function, the control function, the interface function, the protection function, the communication function and the structure function.

Axiom 17: In a mechatronic system, process and control information is transformed alternately in a hierarchical pattern of systems and subsystems.

Axiom 18: If a transformation-function structure representing a mechatronic system includes one or more multi-state elements, then it is possible to substitute these functions by a state-transition structure and a continuous-transformation structure for each state of the system.

Axiom 19: The state transition behavior of a mechatronic system is determined by the structure of control components and their programmable instructions. Control components realize the logical relations between purpose functions on the same and different levels of the causal chain of functions and means.

5 REFERENCES

[1] Klir, J. & Valach, M. (1967) Cybernetic modelling, *Iliffe Books*. London.

[2] Chestnut, H. (1967) Systems engineering methods. *John Wiley*, New York.

[3] Hall, A.D. (1962) A methodology for systems engineering. *Van Nostrand*, Princeton.

[4] Nam Pyo Suh (2001) Axiomatic design – Advances and applications. *Oxford University Press*.

[5] Julie Hirtz, et al. (2002) A functional basis for engineering design: Reconciling and evolving previous efforts. *Research in Engineering Design*, (2002) 13, pp. 65–82

[6] Rosenman, M. A. and Gero, J. S. (1998) CAD modeling in multidisciplinary design domains, in I. Smith (ed.), Artificial Intelligence in Structural Engineering, *Springer*, Berlin, pp.335-347.

[7] Pahl, G. & Beitz, W. (1988) Engineering design – A systematic approach, The Design Council, *Springer-Verlag*, Berlin.

[8] Hubka, V. & Eder, W.E. (1984) Theory of technical systems, *Springer-Verlag*, New York.

[9] Andreasen, M.M. (1980) Syntesemetoder pa systemgrundlag. Dissertation, *Lunds Tekniska Hogskola*.

[10] Tjalve, E. (1979) A short course in industrial design. *Newnes-Butterworth*, London.

[11] Murali Jayaram, Li Chen: Functional modeling of complex mechatronic system. *DETC2003/DTM-48636.*

[12] Li Ruiqin (2004) Research on design theory and methods of scheme design for mechatronic system [D]. *Shanghai Jiaotong University*.

Authors' Address:
Xu Yong
Zou Huijun
Shanghai Jiatong University
School of Mechanical Engineering
Huashan Road, 1954
Shanghai, China
brucexuyong@163.com

Prejeto:
Received: 6.6.2006

Sprejeto:
Accepted: 21.2.2007

Odprto za diskusijo: 1 leto
Open for discussion: 1 year

Strojniški vestnik - Journal of Mechanical Engineering 53(2007)4, 253-264
UDK - UDC 620.178.3:669.1
Strokovni članek - Speciality paper (1.04)

Določevanje parametrov utrujanja jekla z veliko trdnostjo S1100Q

Determination of the Low-Cycle Fatigue Parameters of S1100Q High-Strength Steel

Marko Knez - Janez Kramberger - Srečko Glodež
(Fakulteta za strojništvo, Maribor)

V prispevku je predstavljena preizkusna raziskava za določitev utrujenostnih parametrov jekla z veliko trdnostjo S1100Q, ki se z namenom zmanjšanja skupne teže, pogosto uporablja pri zelo obremenjenih strojnih delih in konstrukcijah (premični žerjavi). Preizkusi so izvedeni v režimu malocikličnega utrujanja po standardu ASTM E 606 z nespremenljivim premerom preizkušanca. Na podlagi izsledkov preizkusa so po predpisani računski metodi po ASTM E 606 določeni ustrezni parametri malocikličnega utrujanja.

V drugem delu prispevka je predstavljen računski model za določitev dobe trajanja nosilnega droga protiuteži premičnega žerjava. Računski model temelji na deformacijski metodi (ε-N), pri čemer so uporabljene poprej določene snovne lastnosti jekla z veliko trdnostjo S1100Q. Na posebej izvedenem hidravlično vodenem utripnem stroju so izvedeni tudi utrujenostni preizkusi nosilnega droga. Primerjava med računskimi in preizkusnimi izsledki kaže dobro ujemanje.

(Ključne besede: utrujanje materialov, doba trajanja, numerični izračuni, deformacijske metode)

We designed an experimental investigation to determine the fatigue properties of the high-strength steel S1100Q, which is often used in highly loaded machine components and structures, e.g., mobile cranes, to reduce weight. Fatigue tests were carried out in a low-cycle regime according to the ASTM E 606 standard, where standardized, uniform-gauge test specimens are used. On the basis of the experimental results the appropriate low-cycle fatigue parameters were determined using the calculation procedure described in ASTM E 606.

In the second part of the paper, a service-life evaluation of the counterweight of a mobile crane by means of a computational analysis is presented. The computational analysis was performed using the local strain-life approach (ε-N), where the appropriate material properties for treated high-strength S1100Q steel were used. The experimental fatigue tests on the bars were carried out in a specially constructed hydraulic pulsation test machine. The comparison of the computational and experimental results showed a reasonable agreement.

(Keywords: fatigue, life times, numerical calculations, strain-life approach)

0 UVOD

Pri dimenzioniranju dinamično obremenjenih strojnih delov in konstrukcij postaja vse bolj pomembna napoved njihove dobe trajanja. Pri mnogih konstrukcijah (npr. premični žerjavi) so vedno večje tudi zahteve po zmanjšanju njihove skupne teže. Ena od možnosti za dosego tega cilja je zmanjšanje nosilnih prečnih prerezov z uporabo jekel z veliko trdnostjo, pri čemer je treba uporabiti ustrezne konstrukcijske rešitve, ki zmanjšujejo možnost nastanka utrujenostnih poškodb. Če se le-

0 INTRODUCTION

When it comes to the design of cyclically loaded engineering structures and components, the prediction of their service life is of great importance. There is a growing interest in many structures, for example, mobile cranes, in order to reduce the weight of the structure. One way to achieve this goal is to reduce the required cross-sections using high-strength steel. Thus, clear design guidelines are needed to ensure that fatigue failures are avoided in critical cross-sections. Apart from the design of new te pojavijo, je treba znati oceniti preostalo dobo trajanja konstrukcije.

Izračun dobe trajanja dinamično obremenjenih komponent temelji na poznavanju napetosti oziroma deformacij v kritičnih prečnih prerezih, ki jih običajno določimo numerično po metodi končnih elementov (MKE). Glavne vplivne veličine na dobo trajanja so zunanje obremenitve in trdnostne lastnosti uporabljenega materiala. To pomeni, da je za tovrstne preračune treba poznati trdnostne lastnosti materiala pri utrujevalnih obremenitvah.

Za reševanje problemov utrujanja se dandanes vse več uporablja deformacijska metoda ([1] in [2]), še posebej pri dimenzioniranju dinamično obremenjenih komponent ob navzočnosti raznih zarez. Če je strojni del z zarezo izpostavljen dinamični obremenitvi, je obnašanje materiala mogoče opisati s poznavanjem deformacij ob zarezi. Predvsem v primeru plastifikacije materiala je določitev deformacij preprostejša kakor določitev ustreznih napetosti. Napovedovanje utrujenostnih poškodb z deformacijsko metodo se v takšnih primerih nanaša predvsem na krajevne deformacije ob zarezi in dejansko pomeni določitev števila nihajev obremenitve za nastanek razpoke. Za celotno rešitev problema je mimo lokalnih deformacij ob zarezi treba poznati tudi ustrezne parametre malocikličnega utrujanja uporabljenega materiala.

Slika 1 prikazuje deformacijske krivulje v dvojnem logaritemskem diagramu, kjer je N_f število nihajev do pojava poškodbe. Skupna amplitudna deformacija ε_a na sliki 1 sestoji iz elastične ($\Delta\varepsilon_e/2$) in plastične ($\Delta\varepsilon_p/2$) amplitudne deformacije, ki jih preberemo iz stabilnih histereznih zank. Pri določenem številu nihajev N_f je skupna deformacija vsota elastične in plastične deformacije ([1] in [2]):

structures, there is also an increasing interest in assessing the remaining fatigue life of existing structures.

The service-life calculation of a cyclically loaded component is based on a knowledge of the stresses or deformations in the critical cross-sections, usually calculated by means of a finite-element analysis (FEA). The main parameters influencing the fatigue life are the external loads and the strength behavior of the material. Therefore, the appropriate fatigue properties of the material should be known for such an analysis.

The strain-based approach to fatigue problems is widely used at present ([1] and [2]). The most common application of the strain-based approach is in the fatigue of notched members. In a notch component subjected to cyclic external loads, the behavior of the material at the root of the notch is best considered in terms of strain. As long as there is an elastic constraint surrounding a local plastic zone at the notch, the strains can be calculated more easily than the stress. Since fatigue damage is assessed directly in terms of local strain, this approach is also called the "local strain approach". A reasonable expected fatigue life, based on the nucleation or formation of small macrocracks, can then be determined if one knows the local strain-time history at a notch in the component and the unnotched strain-life fatigue properties of the material.

Strain-life fatigue curves plotted on log-log scales are shown schematically in Fig. 1, where N_f is the number of cycles to failure. The total strain amplitude, ε_a, shown in Fig.1 has been resolved into the elastic ($\Delta\varepsilon_e/2$) and the plastic ($\Delta\varepsilon_p/2$) strain components from the steady-state hysteresis loops. At a given life N_f the total strain is the sum of the elastic and plastic strains, as follows ([1] and [2]):

$$\varepsilon_a = \frac{\Delta\varepsilon_e}{2} + \frac{\Delta\varepsilon_p}{2} = \frac{\sigma_f'}{E} \cdot \left(2 \cdot N_f\right)^b + \varepsilon_f' \cdot \left(2 \cdot N_f\right)^c \quad (1),$$

kjer so E modul elastičnosti, σ_f' koeficient trdnosti pri utrujanju, b eksponent trdnosti pri utrujanju, ε_f' koeficient žilavosti pri utrujanju in c eksponent žilavosti pri utrujanju. Utrujenostne parametre σ_f', b, ε_f' in c, ki jih imenujemo tudi "parametri malocikličnega utrujanja", določimo s preizkusi po standardu ASTM E 606 [3]. Če je pri dejanskem strojnem delu ali konstrukciji poznana skupna amplitudna deformacija ε_a (ki jo določimo numerično ali z meritvami), določimo dobo trajanja N_f z ponavljajočim postopkom po enačbi (1).

where E is the modulus of elasticity, σ_f' is the fatigue-strength coefficient, b is the fatigue-strength exponent, ε_f' is the fatigue-ductility coefficient and c is the fatigue-ductility exponent. The strain-life fatigue properties σ_f', b, ε_f' and c, which are often referred to as the "low-cycle fatigue properties", are obtained experimentally according to the ASTM E 606 standard [3]. When the total strain amplitude, ε_a, in real machine part or structure is known (it can be measured or determined numerically), the fatigue life N_f can then be calculated iteratively using Equation (1).

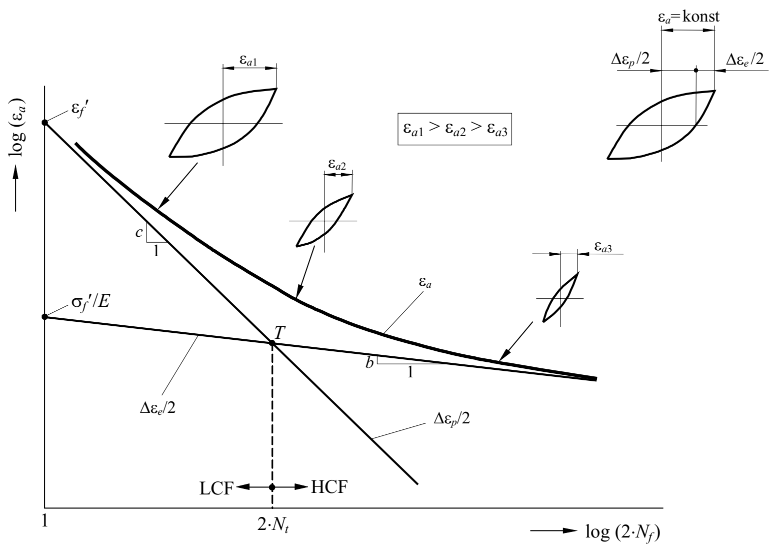

Sl. 1. *Deformacijske krivulje s prikazom skupne (ε_a), elastične ($\Delta\varepsilon_e/2$) in plastične ($\Delta\varepsilon_p/2$) amplitudne deformacije*

Fig. 1. *Strain-life curves showing total (ε_a), elastic ($\Delta\varepsilon_e/2$) and plastic ($\Delta\varepsilon_p/2$) strain amplitude*

1 PARAMETRI MALOCIKLIČNEGA UTRUJANJA JEKLA Z VELIKO TRDNOSTJO S1100Q

Določevanje parametrov malocikličnega utrujanja σ_f', b, ε_f' in c je standardizirano po standardu ASTM E 606 [3], ki predpisuje natančna priporočila glede testnih preizkušancev, preizkusnega stroja s pripadajočo opremo, poteka preizkušanja in končnega poročila.

Preizkušani material S1100Q je bil dobavljen v obliki vroče valjanih plošč, iz katerih so bili v smeri valjanja izrezani surovci ustreznih izmer. Iz teh so bili z mehansko obdelavo izdelani končni preizkušanci na sliki 2.

Preglednica 1 podaja kemijsko sestavo preizkušanega gradiva, na sliki 3 pa je prikazana mikrostruktura gradiva. S slike je razvidno, da je

1 LOW-CYCLE FATIGUE PROPERTIES OF THE HIGH-STRENGTH STEEL S1100Q

The determination of the low-cycle fatigue properties σ_f', b, ε_f' and c is standardized according to the ASTM E 606 standard [3], which provides detailed recommendations about the test specimens, the testing machine with appropriate equipment, the testing procedure and the final report.

The investigated material S1100Q was supplied as hot-rolled plates. Appropriate sizes of raw material were cut out of the plate in the rolling direction. Further specimens were machined to the final shape shown in Fig. 2.

Table 1 shows the chemical composition of the tested material. The material microstructure is shown in Fig. 3. It is evident that the structure

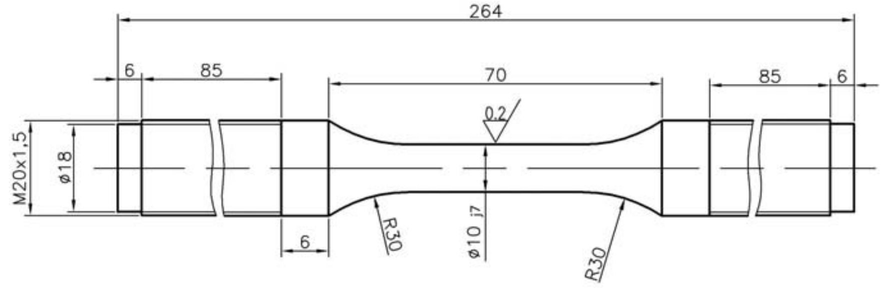

Sl. 2. *Testni preizkušanec po standardu ASTM E 606*

Fig. 2. *Test specimen according to ASTM E 606 standard*

Preglednica 1. *Kemijska sestava jekla z veliko trdnostjo S1100Q*
Table 1. *Chemical composition of high strength steel S1100Q*

Element	C	Si	Mn	P	S	Cr	Ni	Mo	V	Cu	Al	Nb	N	B
%	0,18	0,2	0,83	0,007	0,003	0,56	1,88	0,564	0.057	0,01	0,61	0,017	0,006	0,002

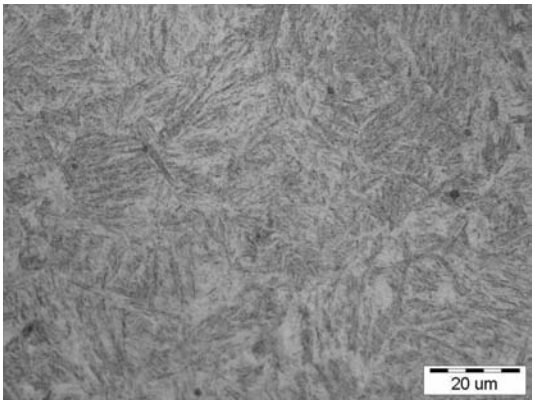

Sl. 3. *Mikrostruktura materiala*
Fig. 3. *Microstructure of the material*

struktura gradiva igličasti bainit z zelo drobnimi iglicami. Zaradi različne usmerjenosti rasti posameznih kristalov je moč predpostaviti povprečne mehanske lastnosti v vseh smereh obravnavane sestave.

Pred utrujenostnimi preizkusi je bil izveden statični natezni preizkus z enakim preizkušancem kakor ga prikazuje slika 2. Slika 4*a* prikazuje tehnični diagram napetost - deformacija, iz katerega so določeni natezna trdnost R_m = 1450 MPa, meja plastičnosti R_e = 1148 MPa in modul elastičnosti gradiva E = 194889 MPa. Iz dejanskega diagrama napetost - deformacija na sliki 4*b* pa sta ob upoštevanju dejanske napetosti σ in dejanske plastične deformacije ε_p iz Hollomonovega razmerja (2) določena trdnostni koeficient K =2272 MPa in deformacijski eksponent utrjanja n = 0,109. Pri tem je predpostavljeno, da je razmerje med dejansko napetostjo in plastično deformacijo v dvojnem logaritemskem diagramu linearno, kjer pomenita K napetost pri ε_p = 1, n pa strmino premice (sl. 5).

resembles lower needle bainite with extremely fine needles. Because of the different orientations of crystal growth it can be assumed that the average mechanical properties can be used in all loading directions.

Before the fatigue tests, the monotonic tensile test was made using the same specimen as shown in Fig. 2. The engineering stress-strain curve is shown in Fig. 4*a*, from which the ultimate tensile strength R_m = 1450 MPa, the yield stress R_e = 1148 MPa and the modulus of elasticity E = 194889 MPa are recorded. Considering the true stress, σ, and true plastic strain, ε_p, from the true stress-strain curve in Fig. 4*b*, the strength coefficient K =2272 MPa and the strain-hardening exponent n = 0.109 were determined using the Hollomon relationship (2). Here it is assumed that the plot of true stress versus true plastic strain in log-log coordinates results in a linear curve, where K is the stress intercept at ε_p = 1 and n denotes the slope of the line (see Fig. 5).

$$\sigma = K \cdot (\varepsilon_p)^n \qquad (2).$$

Utrujenostni preizkusi so bili izvedeni z nadzorom deformacije na hidravličnem preizkusnem stroju za utrujanje Instron 1255 (slika 6) z računalniškim vmesnikom in sistemom zbiranja podatkov Instron 8500. Nihaj obremenitve je imel trikotno obliko z obremenitvenim razmerjem $R = -1$. Temperatura preizkušanja 20 °C je bila med

The low-cycle fatigue tests were carried out in the strain-controlled regime on an Instron 1255 servo-hydraulic fatigue machine (see Fig. 6) with a computer-aided control unit and an Instron 8500 data-recording system. The loading waveform was triangular with a loading ratio $R = -1$. The specimen temperature was 20°C and this was manually checked

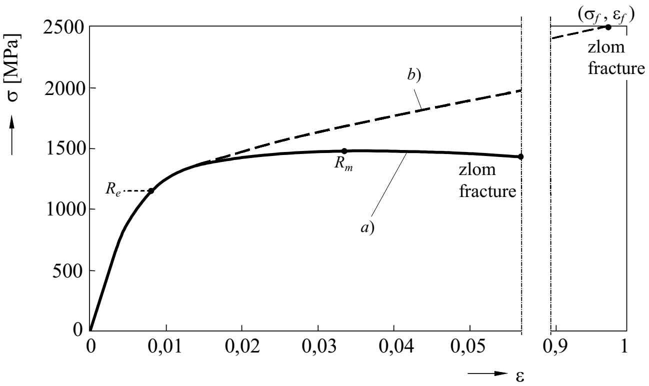

Sl. 4. *Tehnična (a) in dejanska (b) krivulja napetost - deformacija*
Fig. 4. *The engineering (a) and true (b) stress-strain curve*

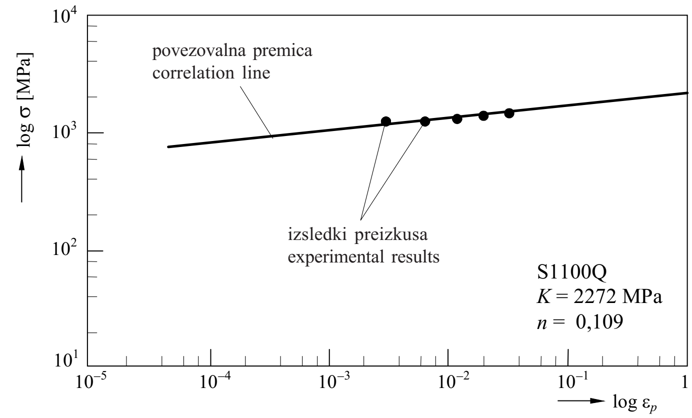

Sl. 5. *Razmerje med dejansko napetostjo in dejansko plastično deformacijo*
Fig. 5. *True stress versus true plastic strain behaviour*

Sl. 6. *Preizkusni stroj INSTRON 1255*
Fig. 6. *Test machine INSTRON 1255*

preizkusom nadzorovana ročno z digitalnim termometrom. Frekvenca obremenjevanja je bila višja pri nižjih amplitudnih deformacijah, saj je nastala energija v tem primeru manjša. Parametri malocikličnega utrujanja so bili določeni na podlagi rezultatov osmih preizkušancev, pri čemer je bil kriterij poškodbe zlom preizkušanca.

during the test procedure using a digital thermometer. The loading frequency was higher for specimens with a lower deformation amplitude, as the energy generated in each cycle is lower. The low-cycle fatigue parameters were determined using the results from 8 specimens, where specimen separation was chosen as the failure criterion.

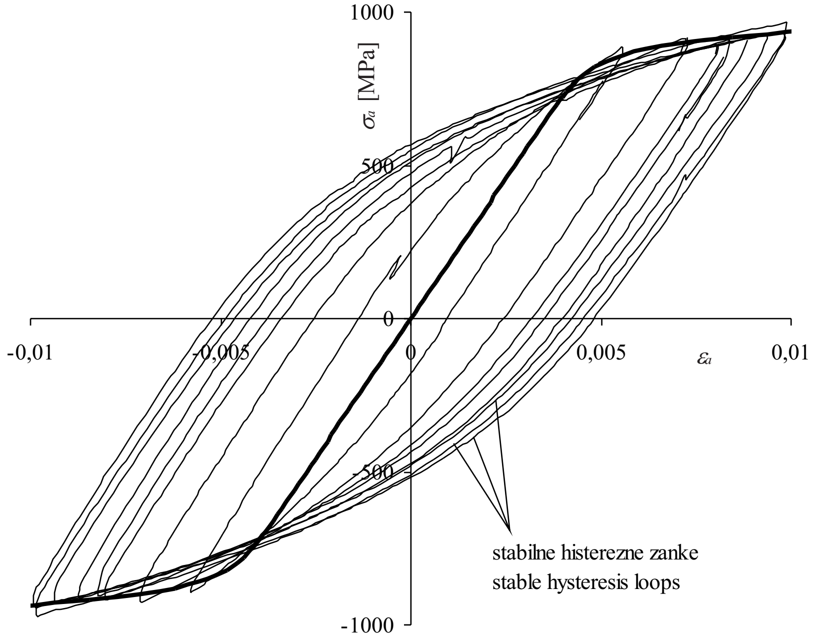

Sl. 7. *Ciklični diagram napetost - deformacija*
Fig. 7. *The cyclic stress-strain curve*

Slika 7 prikazuje ciklično krivuljo napetost - deformacija, ki je dobljena na podlagi osmih histereznih zank, ki opisujejo utrujenostno obnašanje preizkušancev na različnih deformacijskih ravneh. Iz diagrama na sliki 7 sta določena ciklični modul elastičnosti E' = 183443 MP in ciklična meja plastičnosti R_e' = 875 MPa.

Podobno kakor pri statičnem je tudi pri utrujenostnem preizkusu odvisnost med dejansko amplitudno napetostjo σ_a in dejansko amplitudno deformacijo $\Delta\varepsilon_p/2$ v dvojnem logaritemskem diagramu linearna (sl. 8) in jo izrazimo z eksponentno enačbo:

Fig. 7 shows the cyclic stress-strain curve, which is constructed on the basis of 8 stable hysteresis loops describing the fatigue behavior of the specimens loaded on a different strain level. From Fig. 7, the cyclic modulus of elasticity, E' = 183443 MPa, and the cyclic yield stress, R_e' = 875 MPa, are recorded.

Similar to the monotonic deformation in a tension test, a plot of the true stress amplitude, σ_a, versus the true plastic-strain amplitude, $\Delta\varepsilon_p/2$, in log-log coordinates results in a linear curve (see Fig. 8) represented by the power function

$$\sigma = K' \cdot \left(\frac{\Delta\varepsilon_p}{2}\right)^{n'} \qquad (3),$$

kjer sta K' trdnostni koeficient in n'deformacijski eksponent utrjanja pri dinamični obremenitvi. S slike 8 se vidi, da je K' = 1280 MPa (pripadajoča napetost pri $\Delta\varepsilon_p/2 = 1$) in n' = 0,059 (strmina premice).

Slika 9 prikazuje krivulje dobe trajanja v dvojnem logaritemskem diagramu, kjer pomeni N_f število nihajev do zloma preizkušanca. Če primerjamo dobljene veličine na sliki 9 s teoretičnimi veličinami na sliki 1, sledijo parametri malocikličnega utrujanja za jeklo z veliko trdnostjo S1100Q:

- koeficient trdnosti pri utrujanju: σ_f' = 2076 MPa
- eksponent trdnosti pri utrujanju: b = –0,0997
- koeficient žilavosti pri utrujanju: ε_f' = 9,93
- eksponent žilavosti pri utrujanju: c = –0,978

where K' is the cyclic strength coefficient and n' is the cyclic strain-hardening exponent. It is evident from Fig. 8 that K' = 1280 MPa (stress intercept at $\Delta\varepsilon_p/2 = 1$) and n' = 0.059 (the slope of the line).

Fig. 9 shows the strain-life fatigue curves plotted on log-log scales, where N_f is the number of cycles to failure for each tested specimen. If the magnitudes in Fig. 9 are compared with the theoretical ones in Fig. 1, the low-cycle fatigue parameters for the high-strength steel S1100Q result in:

- fatigue-strength coefficient: σ_f' = 2076 MPa
- fatigue-strength exponent: b = –0,0997
- fatigue-ductility coefficient: ε_f' = 9,93
- fatigue-ductility exponent: c = –0,978

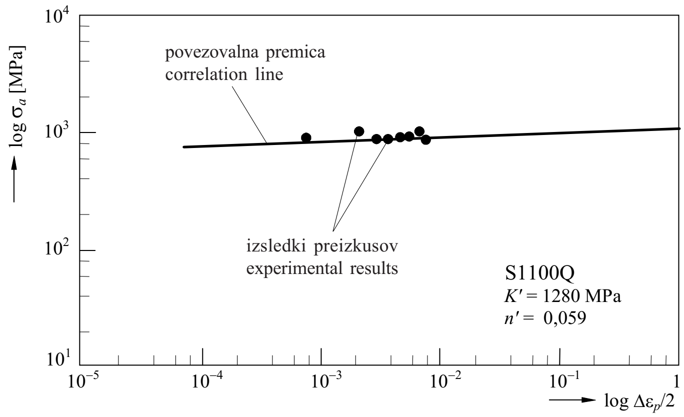

Sl. 8. *Razmerje med dejansko amplitudno napetostjo in dejansko amplitudno plastično deformacijo*
Fig. 8. *True stress amplitude versus true plastic strain amplitude behaviour*

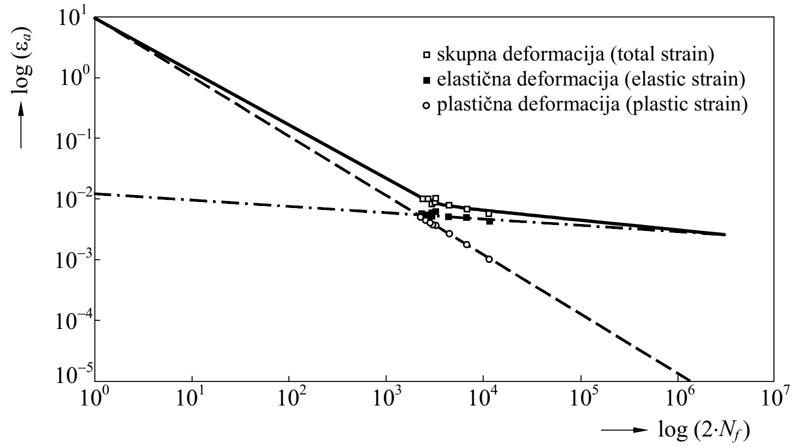

Sl. 9. *Deformacijske krivulje jekla z veliko trdnostjo S1100Q*
Fig. 9. *Strain-life curves of high strength steel S1100Q*

2 PRAKTIČNI PRIMER

Pri goseničnih žerjavih (slika 10) so potrebne protiuteži pogosto obešene na jeklenih verigah. Slednje sestavljajo s sorniki povezani drogovi, običajno izdelani iz jekel z veliko trdnostjo, na primer S1100Q [4]. Na podlagi parametrov malocikličnega utrujanja, določenih v poglavju 1, je v nadaljevanju analizirano obnašanje navedenih drogov pri utrujenostni obremenitvi. Problem je analiziran preizkusno in računsko.

2.1 Izvedeni preizkusi

Preizkusi utrujanja drogov so bili izvedeni na namenski preizkusni napravi, sestavljeni iz dveh togih plošč, povezanih s palično konstrukcijo (sl. 11*a*). Potrebna sila preizkušanja je dosežena prek hidravličnih valjev na osnovni plošči. Velikost sile je

2 PRACTICAL EXAMPLE

Crawler cranes (Fig. 10) are devices in which a counter weight is usually supported by a steel chain, which consists of a series of highly loaded bars, usually made of high-strength steels like S1100Q [4]. On the basis of the low-cycle fatigue parameters determined in Section 1, the fatigue assessment of such steel bars is analysed using experimental testing and computational analysis, as described in the following sections.

2.1 Experimental testing

The fatigue tests were carried out in a specially designed testing machine made of two basic rigid plates, which are connected with a central lattice (Figure 11*a*). The load is applied using the oil pressure pumped into hydraulic cylinders, which are

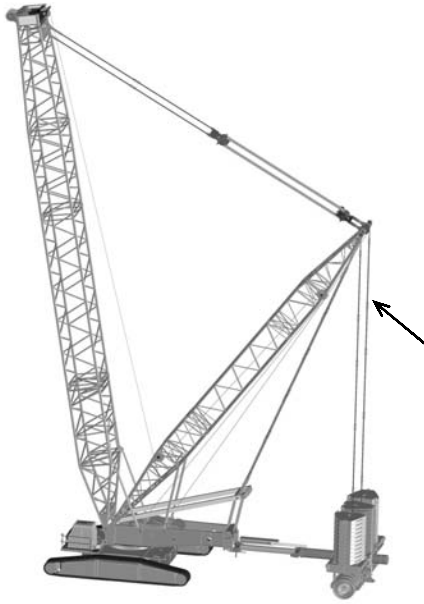

Sl. 10. *Gosenični žerjav*
Fig. 10. *Crawler crane*

določena posredno prek tlaka olja v hidravličnem sistemu. S spremembo smeri pretoka olja je krmiljena smer delovanja sile. Navedena preizkusna naprava omogoča hkrati simultano preizkušanje štirih preizkušancev z največjo natezno silo 1000 kN za vsak preizkušanec. Dejanske napetosti v preizkušancu so nadzorovane prek tlaka olja in še dodatno z merilnimi lističi. Slaba stran preizkusne naprave so potrebne velike sile za dosego želenih napetosti ter težave pri zagotavljanju želenih frekvenc preizkušanja.

Preizkusni drogovi (sl. 11*b*) imajo pravokotni prerez (30×50 mm) in so sklenjeni v obliki ušes z izvrtino za sornik. 6 m dolgi drogovi so iz osnovnih plošč izrezani s plamenskim rezanjem, vse površine rezanja pa so pozneje obdelane z brušenjem. Pri preizkusu so drogovi obremenjeni na nateg, pri čemer je zasledovana natezna napetost v kritičnem prerezu droga.

Za zbiranje podatkov je uporabljena ustrezna oprema "National Instruments". Celotni sistem vsebuje kartico zbiranja podatkov AT-MIO-16E-2, vgrajeno v računalnik, modul za analizo signalov SCXI-1520 in programski paket Lab VIEW 6.1. Modul za analiziranje signalov omogoča sprejem do 8 signalov z merilnih lističev pri frekvencah do 300 kHz. Za končno vrednotenje poteka testiranja je treba podati natančno obliko nihaja obremenitve (največja in najmanjša obremenitev znotraj nihaja). Zaradi velike dolžine kablov (približno 12 m) so uporabljeni 350 Ω merilni

mounted on the base plate. The oil pressure provides a simple means of measuring the applied force. Changing the direction of the load is done by reversing the oil flow with electrical control. The machine can test four bars simultaneously, with a 1000-kN maximum tensile force in each bar. The actual stresses were controlled by means of the oil pressure and checked using strain gauges. The loading machine has certain disadvantages, like the need for large forces to achieve the necessary stresses and the difficulty in providing a high testing frequency.

The testing bar (Figure 11*b*) had a rectangular cross-section (30×50 mm). Each side of the bar contains a head with a hole for a bolt. The fabrication of approximately 6-m-long bars was carried out under normal production procedure, i.e., gas cutting. The grinding was done on gas-cut surfaces. The bars were loaded in tension so that the nominal applied stress was controlled in the critical cross-section.

Equipment produced by National Instruments was used for the data acquisition. The system consists of an AT-MIO-16E-2 multifunction data-acquisition card, running in a PC, with a signal-conditioning module SCXI-1520 and Lab VIEW 6.1 software. This module enables the acquisition of up to 8 signals from strain gauges at a sampling rate of up to 300 kHz. The fatigue analysis and the fatigue testing require an accurate description of the peaks and valleys in the load history. Due to long cables (approximate 12 m), 350 Ω strain gauges and a six-

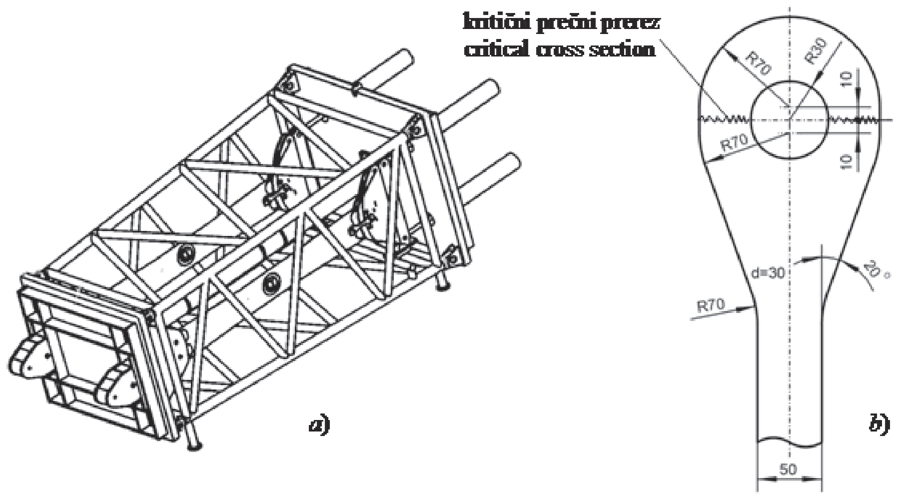

Sl. 11. *Utrujenostna testna naprava (a) in testni preizkušanec (b)*
Fig. 11. *Fatigue testing machine (a) and testing bar (b)*

lističi s šestimi kabelskimi priključki. Dodana sta še dva dodatna kabla za kalibriranje, tako da je ocenjena napaka meritev manjša od enega odstotka.

wire connection were used. An additional two wires were used for the shunt calibration. It is estimated that the measurement error was less than 1%.

2.2 Računska analiza

Računska analiza je potekala v dveh korakih. V prvem je s programskim paketom Abaqus 6.4 [5] numerično po MKE določeno napetostno in deformacijsko polje v kritičnem prečnem prerezu droga. Pri numerični analizi sta bila uporabljena numerični model na sliki 12*a* in vzorec obremenitve na sliki 12*b*. Vzorec obremenitve na sliki 12*b* je enak kakor pri poprej opisanih testnih preizkusih.

V naslednjem koraku je izvedena analiza utrujanja s programskim paketom FE-Safe [6]. Analiza utrujanja je zasnovana na deformacijski metodi (ε-N), pri čemer je za določitev števila nihajev obremenitve N_f do pojava utrujenostne poškodbe v kritičnem prečnem prerezu droga uporabljena Coffin-Mansonova enačba z Morrowo popravo vpliva srednje napetosti [7]:

2.2 Computational analysis

The computational analysis was made in two steps. First, a stress and deformation field in the critical cross-section of the bar was determined numerically using the FEM program code Abaqus 6.4 [5]. The FE model shown in Fig. 12*a* and the loading pattern shown in Fig. 12*b* were used in the computational analysis. Here, the loading pattern in Fig. 12*b* is the same as that used in the experimental testing, described previously.

In the next steep, the fatigue analysis was performed using the FE-Safe program code [6]. The fatigue analysis was based on the strain-life method (ε-N), where the Coffin-Manson relationship with a Morrow mean stress correction was used to determine the number of stress cycles, N_f, required for the fatigue failure in a critical cross-section of the treated bar connection [7]:

$$\frac{\Delta\varepsilon}{2} = \frac{(\sigma_f' - \sigma_m)}{E}\left(2N_f\right)^b + \varepsilon_f' \cdot (2N_f)^c \qquad (4),$$

kjer so $\Delta\varepsilon$ dejanska amplitudna deformacija, σ_m srednja napetost ter E, σ_f', ε_f', b in c materialni parametri, opisani v poglavju 1.

where $\Delta\varepsilon$ is the true strain range, σ_m is the mean stress and E, σ_f', ε_f', b and c are material parameters described in Section 1.

2.3 Preizkusni in računski rezultati

Slika 13*a* prikazuje utrujenostni prelom preizkusnega droga. S slike 13*b* je razvidna začetna

2.3 Experimental and computational results

Figure 13*a* shows the fatigue breakage of the tested bar. The fatigue crack was initiated at the edge

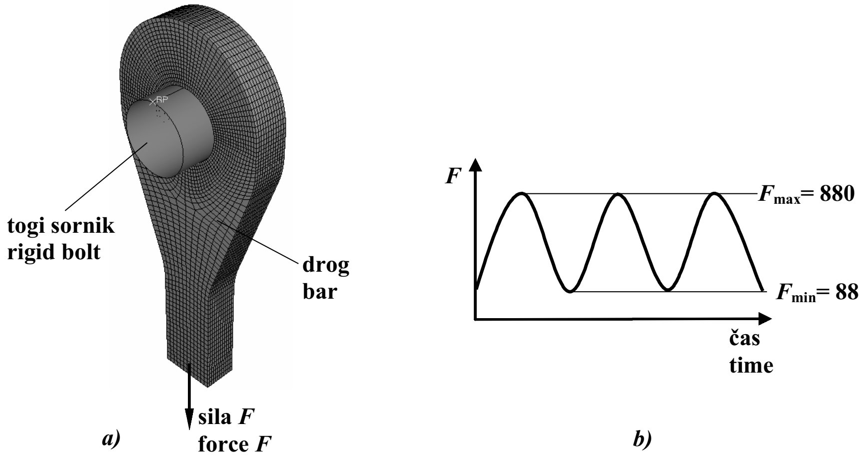

Sl. 12. *Numerični model (a) in vzorec obremenitve (b)*
Fig. 12. *Numerical model (a) and loading pattern (b)*

razpoka na robu izvrtine, ki se je z nadaljnjim utrujanjem širila do končnega zloma v kritičnem prerezu preizkusnega droga. Število nihajev obremenitve N_f do končnega zloma je razvidno iz preglednice 2.

Slika 14 prikazuje porazdelitev napetosti in deformacij vzdolž kritičnega prereza droga, ki so bile upoštevane pri analizi utrujanja s programskim paketom FE-Safe. S slike je razvidno, da se pojavljajo največje napetosti in deformacije v sredini droga, kar je v nasprotju z rezultati preizkusov, pri katerih so se začetne razpoke pojavile na površini preizkušancev. Domnevno so začetne površinske razpoke posledica plamenskega rezanja pri izdelavi testnih preizkušancev. Čeprav so bili preizkušanci po plamenskem rezanju še dodatno obdelani z brušenjem, le-to ni v zadostni meri odpravilo površinskih nepravilnosti (površinska hrapavost, mikrorazpoke, vključki itn.), na katera so jekla z veliko trdnostjo še posebej občutljiva. Računsko število nihajev obremenitve N_f do končnega zloma navaja preglednica 2.

of the hole, which can be seen from Figure 13*b*. The initial crack then propagates until the final fracture in the critical cross-section. The number of stress cycles, N_f, required for the final fracture is shown in Table 2.

Figure 14 shows the stress and strain distribution along the critical cross-section of the bar, which was used for the fatigue analysis with the FE-Safe program code. It is clear that the maximum stresses and deformations appear in the middle of bar thickness, which is opposite to the experimental testing, where the crack is initiated at the edge of the hole. It can be explained by the fact that the test bar specimens were produced with a thermal cutting process, which results in initial surface damage. Although additional surface grinding was applied, this was apparently not sufficient to alleviate the sensitivity of high-strength steel to notches and other material imperfections (surface roughness, micro-cracks, inclusions etc.). The computational number of stress cycles, N_f, required for final fracture is shown in Table 2.

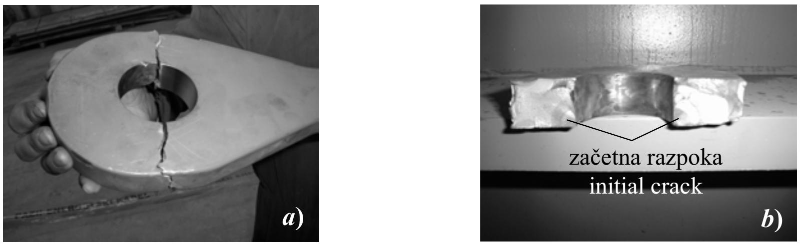

Sl. 13. *Utrujenostni prelom testnega droga (a) in primer prelomne površine (b)*
Fig. 13. *Fatigue breakage of testing bar (a) and example of fracture surface (b)*

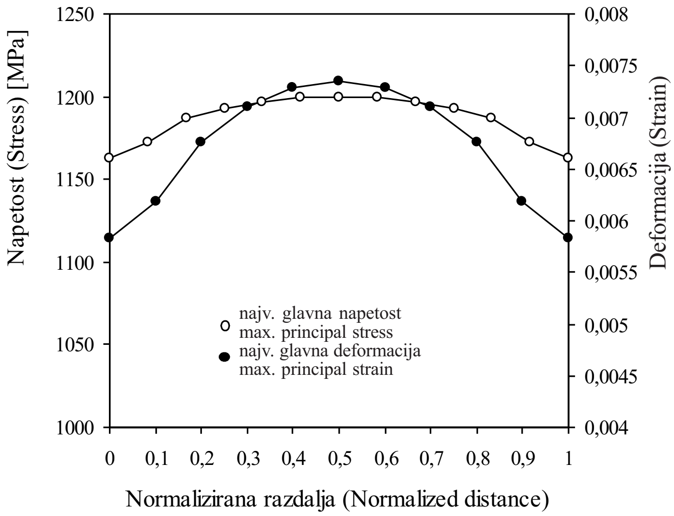

Sl. 14. *Porazdelitev napetosti in deformacije v kritičnem prečnem prerezu droga*
Fig. 14. *Stress and strain distribution in the critical cross section of bar*

Preglednica 2. *Število obremenitvenih ciklov N_f do končne poškodbe*
Table 2. *Number of stress cycles N_f required for final failure*

Preizkusni izsledki Experimental results				Računski izsledki Computational results
Preizkus 1 Test 1	Preizkus 2 Test 2	Preizkus 3 Test 3	Preizkus 4 Test 4	
38029	26727	24795	29036	28705

3 SKLEPI

V podanem prispevku je predstavljena preizkusna določitev parametrov malocikličnega utrujanja jekla z veliko trdnostjo S1100Q. Na temelju utrujenostnih prelomov preizkušancev (prelomna površina poteka poševno pri vseh preizkušancih) lahko povzamemo, da ima preizkušano gradivo dobro utrujenostno trdnost. V primerjavi s statičnim preizkusom je modul elastičnosti pri cikličnem preizkusu manjši za približno 7,5 %. Zaradi razmeroma nizkega eksponenta utrjanja se bo pri utrujenostnih obremenitvah praviloma pojavilo ciklično mehčanje gradiva.

V drugem delu prispevka je predstavljen preizkusni in računski postopek določitve dobe trajanja nosilnega droga protiuteži pri žerjavu. Oba postopka potrjujeta, da je izvrtina za sornik v ušesu droga kritično mesto za nastanek utrujenostne razpoke in pojav končne poškodbe. V preglednici 2 predstavljeni izsledki pomenijo koristne informacije inženirjem pri oceni utrujenostne trdnosti nosilnega droga protiuteži kot pomembnega člena v žerjavnih konstrukcijah.

3 CONCLUSION

We carried out an experimental determination of the mechanical properties and the low-cycle fatigue parameters of the high-strength steel S1100Q. On the basis of the fracture behavior during the fatigue tests (the fracture surface was not in-plane for all the tested specimens) it can be concluded that the investigated material shows good fatigue strength. The modulus of elasticity is, based on fatigue tests, approximately 7.5% lower compared to the monotonic test. Because of the low strain-hardening exponent the cyclic softening of the material is expected as a result of fatigue loading.

In the second part of the paper, the experimental and computational procedure to determine the service life of a counterweight-bar bolted connection is presented. Both procedures show that the connection hole in the bar end is the most critical location for crack initiation and final failure. The results presented in Table 2 are useful information for the designer about a fatigue assessment of a counterweight bar, as an important supporting part for crane structures.

4 LITERATURA
4 LITERATURE

[1] Stephens R.I., Fatemi A., Stephens R.R., Fuchs H.O (2001) Metal fatigue in engineering, *John Wiley & Sons Inc*, New York.
[2] Zahavi E., Torbilo V. (1996) Fatigue design, *CRC Press*, New York.
[3] ASTM E 606 (1998) Standard practice for strain-controlled fatigue testing, *ASTM standard*.
[4] Kramberger J., Potrč I., Bombek G. and Flašker J (2003) Fatigue assessment of high strength steel beam for crawler track cranes, *Gep*, Vol. 10-11, 87-90.
[5] *Abaqus*, Version 6.4, Online documentation, 2003.
[6] *FE-Safe*, Version 5, User's manual, 2003.
[7] Suresh S. (1998) Fatigue of materials, *Cambridge University Press*, Cambridge.

Naslovi avtorjev: Marko Knez
doc. dr. Janez Kramberger
prof. dr. Srečko Glodež
Univerza v Mariboru
Fakulteta za strojništvo
Smetanova 17
2000 Maribor
marko.knez@uni-mb.si
jkramberger@uni-mb.si
srecko.glodez@uni-mb.si

Authors' Address: Marko Knez
Doc. Dr. Janez Kramberger
Prof. Dr. Srečko Glodež
University of Maribor
Faculty of Mechanical Eng.
Smetanova 17
2000 Maribor, Slovenia
marko.knez@uni-mb.si
jkramberger@uni-mb.si
srecko.glodez@uni-mb.si

Prejeto:
Received: 29.8.2006

Sprejeto:
Accepted: 21.2.2007

Odprto za diskusijo: 1 leto
Open for discussion: 1 year

Osebne vesti - Personal Events

Prof. dr. Peter Novak je dopolnil 70 let - Prof. Dr. Peter Novak completed 70 years

Profesor Novak je bil v Strojniškem vestniku zadnjič predstavljen ob njegovi upokojitvi konec leta 1997. Tako smo spoznali njegovo osebno in strokovno življenjsko pot od gimnazijskih let, ki jih je končal leta 1955 na gimnaziji v Novem mestu, zagovora diplome na Fakulteti za strojništvo v Ljubljani pod mentorstvom prof. B. Likarja leta 1961 do pridobljenega naziva rednega profesorja leta 1985. Kljub temu, da smo bili večinoma seznanjeni s poklicnimi dosežki in mnogimi strokovnimi ter družbenimi priznanji, ki jih je prejel v času delovanja na naši fakulteti in poznali profesorja kot neprekosljivega retorika in predavatelja, je mnoge presenetil podatek o njegovih dvestopetdesetih diplomantih, skoraj trideset magistrandih in dvajset doktorandih. Tako priljubljen mentor je bil profesor Novak.

V začetku osemdesetih let je organiziral vrsto obiskov vrhunskih svetovnih strokovnjakov s področja izkoriščanja sončne energije, enem od področij, na katerem je bil pionir v tedanji državi in kasneje postal svetovno priznan strokovnjak. Prizadevanjem o okolju prijazni oskrbi človeštva z energijo je ostal zvest do dandanes.

Ob upokojitvi smo mu sodelavci zaželeli veliko srečnih uric v družbi vnukov. Naša želja se je uresničila in profesor Novak se sedaj lahko zabava in uči s tremi vnuki.

Po desetletju v pokoju pa ostaja profesor Novak eden glavnih ambasadorjev naše stroke. Veseli nas, da tudi to njegovo življenjsko obdobje označujeta osebna in strokovna vitalnost ter vizionarstvo.

V letu 1999 je profesor Novak postal zaslužni član American Society for Heating, Refrigerating and Airconditioning Engineers (ASHRAE). V tem združenju je soustanovitelj skupine za eksergijo (2006) in trenutno vodi pripravo poglavja v knjigi Ashrae Book of Fundamentals o eksergiji. V njem bo obširno predstavljeno, tudi po zaslugi profesor Novaka, delo profesor Ranta. Je podpredsednik Evropskega združenja REHVA in v združenju vodi komisiji za nagrade in raziskave. Skoraj deset let (do 2003) je bil predsednik komisije E1 Klimatizacija in član Znanstvenega sveta v Mednarodnem inštitutu za hlajenje (IIR), svetovni medvladni organizaciji z več kot stoletno tradicijo. Leta 1999 je postal član upravnega odbora in leta 2003 tudi častni član IIR. Od ustanovitve do danes je predsednik komisij za okoljske nagrade in nagrade za energetsko učinkovito podjetje v Sloveniji ter član Usmerjevalnega komiteja za okoljske nagrade EU. Več ko dve desetletji pa je tudi član Sveta R Slovenije za varstvo okolja.

Profesor Novak je pomembno prispeval k razvoju Dolenjske, regije iz katere prihaja. Kot predsednik razvojnega sveta za JV Slovenijo je razvil koncept Univerze v Novem mestu in plod njegovih prizadevanj je leta 2006 ustanovljena Visoka šola za tehnologije in sisteme VITES, katere dekan je.

Dokaz njegovega vizionarstva je prizadevanje za združevanje slovenske industrije sistemov stavbnih strojnih instalacij. Prizadevanje, ki je dobilo največjo potrditev z ustanovitvijo Hidria Inštituta Klima v letu 2006, katerega idejni nosilec je profesor Novak.

Na srečanju, ki ga je v čast profesor Novaka, kot ustanovnega in častnega člana, organiziralo Slovensko društvo za sončno energijo, je imel predavanje o vlogi Združenih narodov pri reševanju energijske krize. Njegova vizija o pravični in trajnostni oskrbi človeštva z energijo je razumljivo še enkrat, tako kakor na številnih mednarodnih konferencah, vzbudila izjemno pozornost.

Profesorju ob sedemdesetletnici želimo veliko veselja v družinskim krogu in uresničitev želje po lepšem in pravičnejšem svetu za vse generacije, ki jo je vedno gojil.

Srečno, profesor Novak !

prof. dr. Sašo Medved

Doktorat in diplome - Doctor's and Diploma Degrees

DOKTORAT

Na Fakulteti za strojništvo Univerze v Mariboru je z uspehom zagovarjala svojo doktorsko disertacijo:

dne *14. marca 2007*: **Alenka Ojstršek**, z naslovom: "Vloga različnih nosilcev biomase pri čiščenju tekstilnih barvalnih odpadnih vod" (mentorji: prof. dr. Milenko Roš, prof. dr. Aleksandra Lobnik, prof. dr. Niko Samec).

S tem je navedena kandidatka dosegla akademsko stopnjo doktorja znanosti.

DIPLOMIRALI SO

Na Fakulteti za strojništvo Univerze v Ljubljani so pridobili naziv univerzitetni diplomirani inženir strojništva:

dne *29. marca 2007*: Matej ČADEŽ, Marjan HUDOKLIN, Jernej KLOPČIČ.

Na Fakulteti za strojništvo Univerze v Mariboru sta pridobila naziv univerzitetni diplomirani inženir strojništva:

dne *29. marca 2007*: Aleš VAUHNIK, Primož ZAJŠEK.

*

Na Fakulteti za strojništvo Univerze v Ljubljani so pridobili naziv diplomirani inženir strojništva:

dne *8. marca 2007*: Štefan LOTRIČ, Andrej MIHELAČ, Samo SAMBOL, Mitja VIRANT;

dne *9. marca 2007*: Marko ARNOLJ, Anže BERTONCELJ, Janez LUKANČIČ, Pavel OBLAK, David PUC, Peter TEHOVNIK, Daniel VIGINI.

Na Fakulteti za strojništvo Univerze v Mariboru so pridobili naziv diplomirani inženir strojništva:

dne *29. marca 2007*: Janez KOSIRNIK, Matjaž ORTHABER, Sebastijan PARADIŽNIK; Tomaž PUKL, Aljoša ŠTRAFELA, Rok TURNŠEK, Danilo VIDERMAN, Slavko ZUPANČIČ.

Navodila avtorjem - Instructions for Authors

Članki morajo vsebovati:
- naslov, povzetek, besedilo članka in podnaslove slik v slovenskem in angleškem jeziku,
- dvojezične preglednice in slike (diagrami, risbe ali fotografije),
- seznam literature in
- podatke o avtorjih.

Strojniški vestnik izhaja od leta 1992 v dveh jezikih, tj. v slovenščini in angleščini, zato je obvezen prevod v angleščino. Obe besedili morata biti strokovno in jezikovno med seboj usklajeni. Članki naj bodo kratki in naj obsegajo približno 8 strani. Izjemoma so strokovni članki, na željo avtorja, lahko tudi samo v slovenščini, vsebovati pa morajo angleški povzetek.

Za članke iz tujine (v primeru, da so vsi avtorji tujci) morajo prevod v slovenščino priskrbeti avtorji. Prevajanje lahko proti plačilu organizira uredništvo. Če je članek ocenjen kot znanstveni, je lahko objavljen tudi samo v angleščini s slovenskim povzetkom, ki ga pripravi uredništvo.

Papers submitted for publication should comprise:
- Title, Abstract, Main Body of Text and Figure Captions in Slovene and English,
- Bilingual Tables and Figures (graphs, drawings or photographs),
- List of references and
- Information about the authors.

Since 1992, the Journal of Mechanical Engineering has been published bilingually, in Slovenian and English. The two texts must be compatible both in terms of technical content and language. Papers should be as short as possible and should on average comprise 8 pages. In exceptional cases, at the request of the authors, speciality papers may be written only in Slovene, but must include an English abstract.

For papers from abroad (in case that none of authors is Slovene) authors should provide Slovenian translation. Translation could be organised by editorial, but the authors have to pay for it. If the paper is reviewed as scientific, it can be published only in English language with Slovenian abstract, that is prepared by the editorial board.

VSEBINA ČLANKA

Članek naj bo napisan v naslednji obliki:
- Naslov, ki primerno opisuje vsebino članka.
- Povzetek, ki naj bo skrajšana oblika članka in naj ne presega 250 besed. Povzetek mora vsebovati osnove, jedro in cilje raziskave, uporabljeno metodologijo dela,povzetek rezulatov in osnovne sklepe.
- Uvod, v katerem naj bo pregled novejšega stanja in zadostne informacije za razumevanje ter pregled rezultatov dela, predstavljenih v članku.
- Teorija.
- Eksperimentalni del, ki naj vsebuje podatke o postavitvi preskusa in metode, uporabljene pri pridobitvi rezultatov.
- Rezultati, ki naj bodo jasno prikazani, po potrebi v obliki slik in preglednic.
- Razprava, v kateri naj bodo prikazane povezave in posplošitve, uporabljene za pridobitev rezultatov. Prikazana naj bo tudi pomembnost rezultatov in primerjava s poprej objavljenimi deli. (Zaradi narave posameznih raziskav so lahko rezultati in razprava, za jasnost in preprostejše bralčevo razumevanje, združeni v eno poglavje.)
- Sklepi, v katerih naj bo prikazan en ali več sklepov, ki izhajajo iz rezultatov in razprave.
- Literatura, ki mora biti v besedilu oštevilčena zaporedno in označena z oglatimi oklepaji [1] ter na koncu članka zbrana v seznamu literature. Vse opombe naj bodo označene z uporabo dvignjene številke[1].

THE FORMAT OF THE PAPER

The paper should be written in the following format:
- A Title, which adequately describes the content of the paper.
- An Abstract, which should be viewed as a mini version of the paper and should not exceed 250 words. The Abstract should state the principal objectives and the scope of the investigation, the methodology employed, summarize the results and state the principal conclusions.
- An Introduction, which should provide a review of recent literature and sufficient background information to allow the results of the paper to be understood and evaluated.
- A Theory
- An Experimental section, which should provide details of the experimental set-up and the methods used for obtaining the results.
- A Results section, which should clearly and concisely present the data using figures and tables where appropriate.
- A Discussion section, which should describe the relationships and generalisations shown by the results and discuss the significance of the results making comparisons with previously published work. (Because of the nature of some studies it may be appropriate to combine the Results and Discussion sections into a single section to improve the clarity and make it easier for the reader.)
- Conclusions, which should present one or more conclusions that have been drawn from the results and subsequent discussion.
- References, which must be numbered consecutively in the text using square brackets [1] and collected together in a reference list at the end of the paper. Any footnotes should be indicated by the use of a superscript[1].

OBLIKA ČLANKA

Besedilo članka naj bo pripravljeno v urejevalnilku Microsoft Word. Članek nam dostavite v elektronski obliki.

Ne uporabljajte urejevalnika LaTeX, saj program, s katerim pripravljamo Strojniški vestnik, ne uporablja njegovega formata.

Enačbe naj bodo v besedilu postavljene v ločene vrstice in na desnem robu označene s tekočo številko v okroglih oklepajih

THE LAYOUT OF THE TEXT

Texts should be written in Microsoft Word format. Paper must be submitted in electronic version.

Do not use a LaTeX text editor, since this is not compatible with the publishing procedure of the Journal of Mechanical Engineering.

Equations should be on a separate line in the main body of the text and marked on the right-hand side of the page with numbers in round brackets.

Enote in okrajšave

V besedilu, preglednicah in slikah uporabljajte le standardne označbe in okrajšave SI. Simbole fizikalnih veličin v besedilu pišite poševno (kurzivno), (npr. *v, T, n* itn.). Simbole enot, ki sestojijo iz črk, pa pokončno (npr. ms^{-1}, K, min, mm itn.).

Vse okrajšave naj bodo, ko se prvič pojavijo, napisane v celoti v slovenskem jeziku, npr. časovno spremenljiva geometrija (ČSG).

Slike

Slike morajo biti zaporedno oštevilčene in označene, v besedilu in podnaslovu, kot sl. 1, sl. 2 itn. Posnete naj bodo v ločljivosti, primerni za tisk, v kateremkoli od razširjenih formatov, npr. BMP, JPG, GIF. Diagrami in risbe morajo biti pripravljeni v vektorskem formatu, npr. CDR, AI.

Pri označevanju osi v diagramih, kadar je le mogoče, uporabite označbe veličin (npr. *t, v, m* itn.), da ni potrebno dvojezično označevanje. V diagramih z več krivuljami, mora biti vsaka krivulja označena. Pomen oznake mora biti pojasnjen v podnapisu slike.

Vse označbe na slikah morajo biti dvojezične.

Preglednice

Preglednice morajo biti zaporedno oštevilčene in označene, v besedilu in podnaslovu, kot preglednica 1, preglednica 2 itn. V preglednicah ne uporabljajte izpisanih imen veličin, ampak samo ustrezne simbole, da se izognemo dvojezični podvojitvi imen. K fizikalnim veličinam, npr. *t* (pisano poševno), pripišite enote (pisano pokončno) v novo vrsto brez oklepajev.

Vsi podnaslovi preglednic morajo biti dvojezični.

Seznam literature

Vsa literatura mora biti navedena v seznamu na koncu članka v prikazani obliki po vrsti za revije, zbornike in knjige:

[1] A. Wagner, I. Bajsić, M. Fajdiga (2004) Measurement of the surface-temperature field in a fog lamp using resistance-based temperature detectors, *Stroj. vestn.* 2(2004), pp. 72-79.
[2] Vesenjak, M., Ren Z. (2003) Dinamična simulacija deformiranja cestne varnostne ograje pri naletu vozila. *Kuhljevi dnevi '03*, Zreče, 25.-26. september 2003.
[3] Muhs, D. et al. (2003) Roloff/Matek Maschinenelemente – Tabellen, 16. Auflage. *Vieweg Verlag*, Wiesbaden.

SPREJEM ČLANKOV IN AVTORSKE PRAVICE

Uredništvo Strojniškega vestnika si pridržuje pravico do odločanja o sprejemu članka za objavo, strokovno oceno recenzentov in morebitnem predlogu za krajšanje ali izpopolnitev ter terminološke in jezikovne korekture.

Avtor mora predložiti pisno izjavo, da je besedilo njegovo izvirno delo in ni bilo v dani obliki še nikjer objavljeno. Z objavo preidejo avtorske pravice na Strojniški vestnik. Pri morebitnih kasnejših objavah mora biti SV naveden kot vir.

PLAČILO OBJAVE

Avtorji vseh prispevkov morajo za objavo plačati prispevek v višini 20,00 EUR na stiskano stran prispevka. Prispevek se zaračuna po sprejemu članka za objavo na seji Uredniškega odbora.

Units and abbreviations

Only standard SI symbols and abbreviations should be used in the text, tables and figures. Symbols for physical quantities in the text should be written in italics (e.g. *v, T, n,* etc.). Symbols for units that consist of letters should be in plain text (e.g. ms^{-1}, K, min, mm, etc.).

All abbreviations should be spelt out in full on first appearance, e.g., variable time geometry (VTG).

Figures

Figures must be cited in consecutive numerical order in the text and referred to in both the text and the caption as Fig. 1, Fig. 2, etc. Pictures may be saved in resolution good enough for printing in any common format, e.g. BMP, GIF, JPG. However, graphs and line drawings sholud be prepared as vector images, e.g. CDR, AI.

When labelling axes, physical quantities, e.g. *t, v, m,* etc. should be used whenever possible to minimise the need to label the axes in two languages. Multi-curve graphs should have individual curves marked with a symbol, the meaning of the symbol should be explained in the figure caption.

All figure captions must be bilingual.

Tables

Tables must be cited in consecutive numerical order in the text and referred to in both the text and the caption as Table 1, Table 2, etc. The use of names for quantities in tables should be avoided if possible: corresponding symbols are preferred to minimise the need to use both Slovenian and English names. In addition to the physical quantity, e.g. *t* (in italics), units (normal text), should be added in new line without brackets.

All table captions must be bilingual.

The list of references

References should be collected at the end of the paper in the following styles for journals, proceedings and books, respectively:

[1] A. Wagner, I. Bajsić, M. Fajdiga (2004) Measurement of the surface-temperature field in a fog lamp using resistance-based temperature detectors, *Stroj. vestn.* 2(2004), pp. 72-79.
[2] Vesenjak, M., Ren Z. (2003) Dinamična simulacija deformiranja cestne varnostne ograje pri naletu vozila. *Kuhljevi dnevi '03*, Zreče, 25.-26. september 2003.
[3] Muhs, D. et al. (2003) Roloff/Matek Maschinenelemente – Tabellen, 16. Auflage. *Vieweg Verlag*, Wiesbaden.

ACCEPTANCE OF PAPERS AND COPYRIGHT

The Editorial Committee of the Journal of Mechanical Engineering reserves the right to decide whether a paper is acceptable for publication, obtain professional reviews for submitted papers, and if necessary, require changes to the content, length or language.

Authors must also enclose a written statement that the paper is original unpublished work, and not under consideration for publication elsewhere. On publication, copyright for the paper shall pass to the Journal of Mechanical Engineering. The JME must be stated as a source in all later publications.

PUBLICATION FEE

For all papers authors will be asked to pay a publication fee prior to the paper appearing in the journal. However, this fee only needs to be paid after the paper is accepted by the Editorial Board. The fee is €20.00 per printed paper page.